Ph.D Synopsis on

"Formulation, Optimization and Evaluation of Anti-osteoporotic Drugs Loaded Nanocarriers for Treatment of Osteoporosis."

By

Patil Pravin Yadav (Reg. No.: FOPH/19)

M. Pharm (Pharmaceutics)

Under the supervision of

Prof. (Dr.) Krutika K. Sawant

Professor of Pharmaceutics

Faculty of Pharmacy,

Kalabhavan Campus,

The Maharaja Sayajirao University of Baroda,

Vadodara-390001,

Gujarat, India.

January – 2023

Introduction:

Osteoporosis is a major public health problem and global healthcare burden characterized by reduction in bone mass and structural deterioration of bone tissue leading to impaired skeletal strength. It has clinical implications because of the morbidity, mortality and treatment cost related with osteoporotic fractures. The dramatical increase in fracture risk with age in both men and women, leads to increase in frailty of bones. About 16 % and 24 % of 50 years or older men and women respectively suffer each year globally. According to statistical survey of International Osteoporosis Foundation, 1 out of 3 women above 50 years age and 1 out of 5 men above 50 years age will suffer osteoporotic fracture in their life worldwide. It is one of the major public health issues which has been estimated to rise from 1.66 million in 1990 to 6.26 million by 2050 [1-4].

A number of drugs and their combination approved for treatment and management of osteoporosis include bisphosphonates, strontium ranelate, teriparatide, selective estrogen receptor modulators, statins etc. [2, 4-6]. **Risedronate sodium (RSNa)** is potent nitrogen containing bisphosphonate which is approved for treatment and prevention of osteoporosis [7]. RSNa has short half-life of only 1.5 hr and has low permeability (belongs to the BCS-III) [8]. Oral bioavailability of RSNa is less than 1% due to its high polarity, hydrophilicity and formation of chelate with calcium ions to make it unabsorbable from GIT [8-10]. Conventionally, oral administration of RSNa possesses GI adverse effect like esophagitis or ulcers or oesophageal erosion, which is associated with injuries of upper GIT [8]. The most dangerous side effect of RSNa is osteonecrosis of jaw, related to tooth extraction and occurs in long term treatment. Recently, statins are also used in the management and treatment of osteoporosis due to their anabolic and anti-resorptive effect by increasing the production of bone morphogenic protiens-2 which helps to increase bone formation [11, 12]. **Atorvastatin calcium (ATO)** exerts beneficial effects on bone by blocking conversion of HMG-CoA to mevalonate that increases the expression of bone morphogenic protein-2 (BMP-2) in osteoblasts, inducing osteoblast differentiation and subsequently stimulating bone formation. The low bioavailability of Atorvastatin (12% orally) is due to its poor aqueous solubility, low dissolution rate and extensive first pass metabolism (belongs to BCS class II) [13, 14]. To overcome the drawbacks associated with the selected drugs, alternative route of drug administration is suggested, that is, transdermal route of drug delivery.

Transdermal drug delivery systems (TDDS) deliver the drug through skin layers at controlled rate to the systemic circulation. The skin forms more attractive and accessible route for systemic drug delivery and has many advantages over conventional route viz. bypass hepatic first pass metabolism, avoids factors that affects the GI absorption of drugs like enzymatic degradation, food-drug interaction, pH etc. and patient compliance [15-18]. Different approaches for enhancement of drug permeation include use of natural oils, enzymes, micelles, liposomes, niosomes, polymeric nanoparticles and glycerosomes [19-22]. Here in this present work, we have worked on drug loaded glycerosomes and polyelectrolyte complex nanoparticles [23, 24]. The prepared nanocarriers (glycerosomes and polyelectrolyte complex nanoparticles) were then incorporated into transdermal patch to increase therapeutic effects of drugs and avoid GI side effects.

1. **Glycerosomes:**

   Glycerosomes are novel vesicular systems for dermal and transdermal drug delivery. Glycerosomes are composed of different phospholipids, cholesterol and high concentration of glycerol. Glycerosomes are flexible vesicular drug delivery systems that contain cholesterol which enhances the lipidic bilayer stability [25, 26]. Glycerol is a harmless and fully acceptable short-chain alcohol that can improve the fluidity and deformability of the vesicular bilayer, thus improving the ability of preparations to penetrate through the skin.

2. **Polyelectrolyte complex nanoparticles (PECN):**

   PECN are formed by combinations of polycationic and polyanionic compounds which are association complexes formed between oppositely charged polyelectrolytes (eg. Polymer-polymer, polymer-drug, polymer-drug-polymer etc.). Generally, oppositely charged polyions undergo electrostatic interactions between them (polycations or polyanions) resulting in the PECN formation. The advantage of PEC nanoparticles is that they can be formed without the use of chemical cross-linking agents, thereby making the synthesis process very simple and straightforward [27-29].

Aim:

The present research work was aimed at the formulation, optimization, and evaluation of selected anti-osteoporotic drugs loaded with nanocarriers in the treatment of osteoporosis. Further, the present research work was aimed to evaluate the enhancement of bioavailability of drugs from prepared nanocarriers by the transdermal route (by formulating a transdermal patch).

Objectives:

The objectives of present work were:

- ✓ To formulate novel nanocarriers (glycerosomes and polyelectrolyte complex nanoparticles) for delivery of selected anti-osteoporotic drugs.
- ✓ To optimize composition and process parameters of the nanocarriers formulation and characterize the physico-chemical properties of nanocarriers.
- ✓ To incorporate anti-osteoporotic drugs loaded novel nanocarriers into transdermal patch and evaluate physicochemical characteristics of transdermal patch.
- ✓ To carry out in vitro studies, ex vivo studies and in vivo studies of drug loaded nanocarriers.
- ✓ To assess the stability of drug loaded nanocarriers and their transdermal patch.

Plan of work:

1. Procurement of drugs, excipients and other chemicals and reagents.

2. Analytical method development of drugs.
3. Formulation development of glycerosomes and PECN.
4. Optimization of formulations using design of experiments.
5. Physicochemical characterisation of nanocarriers.
6. Incorporation of nanocarriers into transdermal patch.
7. Physicochemical characterisation of transdermal patch.
8. In vitro cell line studies.
9. Ex vivo skin permeation studies.
10. In vivo animal studies.
11. Stability studies.

Analytical Techniques:

Analytical technique for Atorvastatin:

A. Estimation of Atorvastatin by UV Visible spectrophotometer:

Aliquots of ATO solution (100 µg/mL) ranging from 0.4 to 1.2 ml were transferred into a series of 10 ml volumetric flask and volume was made up to 10 ml with methanol to get a range from 4 µg/mL to 12 µg/mL. The absorbance of samples was measured at 246 nm against reference blank (Methanol) by UV Visible spectrophotometer [30].

Table-1. Calibration data of ATO in methanol

Conc. (µg/mL)	Absorbance ± SD (n=3)	%RSD
4	0.1561 ± 0.0018	1.165
6	0.2482 ± 0.0023	0.957
8	0.3589 ± 0.0007	0.189
10	0.4581 ± 0.0058	1.282
12	0.5737 ± 0.0081	1.412

Mean SD	Slope	LOD	LOQ
0.0038	0.0523	0.239	0.726

(n=3, ± S.D.)

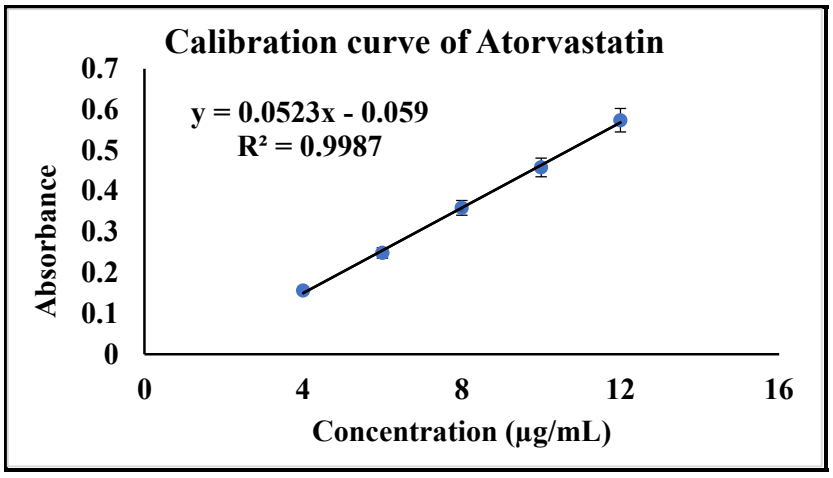

Figure-1. Calibration curve of Atorvastatin in methanol

B. Calibration curve in phosphate buffer (pH 7.4):

Prepared concentrations of 4 to 24 µg/mL from the stock solution of 100 µg/mL and measured absorbance of sample.

Table-2. Calibration data of Atorvastatin in phosphate buffer pH 7.4

Conc. (µg/mL)	Absorbance ± SD (n=3)	%RSD
4	0.152 ± 0.0017	1.14
8	0.296 ± 0.0017	0.586
12	0.441 ± 0.0035	0.796
16	0.599 ± 0.0030	0.509
20	0.751 ± 0.0057	0.768
24	0.903 ± 0.0040	0.447

Mean SD	Slope	LOD	LOQ
0.0033	0.0377	0.288	0.8753

(n=3, ± S.D.)

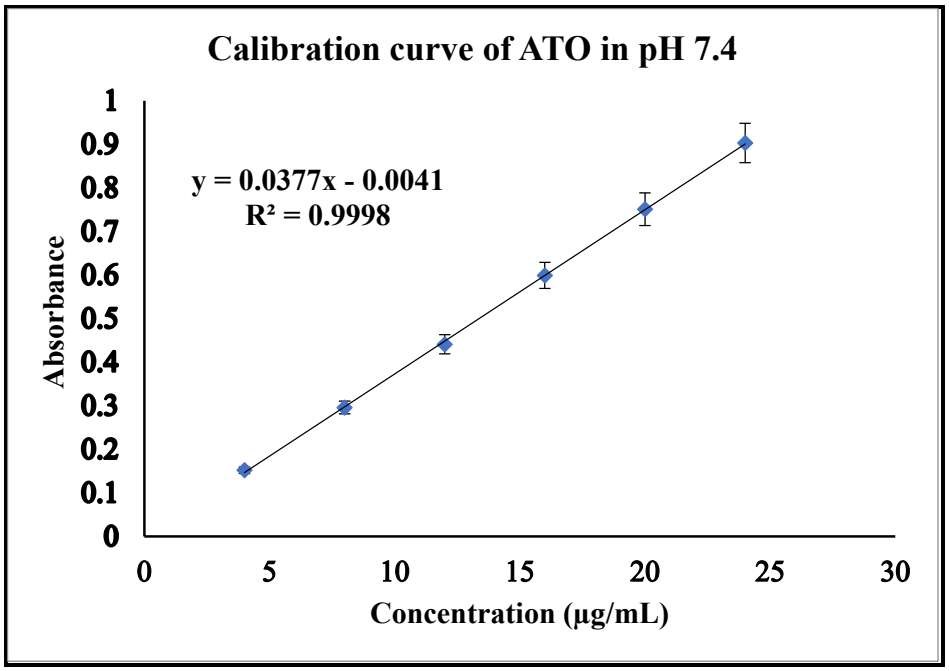

Figure-2. Calibration of Atorvastatin in phosphate buffer pH 7.4

C. Calibration curve in Phosphate buffer (pH 5.5):

Prepared concentrations of 4 to 24 µg/mL from the stock solution of 100 µg/mL and measured absorbance of sample.

Table-3. Calibration data of Atorvastatin in phosphate buffer pH 5.5

Conc. (µg/mL)	Absorbance ± SD (n=3)	%RSD
4	0.154 ± 0.0010	1.120
8	0.333 ± 0.0041	1.240
12	0.510 ± 0.0080	1.580
16	0.691 ± 0.0088	1.280
20	0.885 ± 0.0015	0.172
24	0.958 ± 0.0058	0.605

Mean SD	Slope	LOD	LOQ
0.0050	0.0428	0.385	1.16

(n=3, ± S.D.)

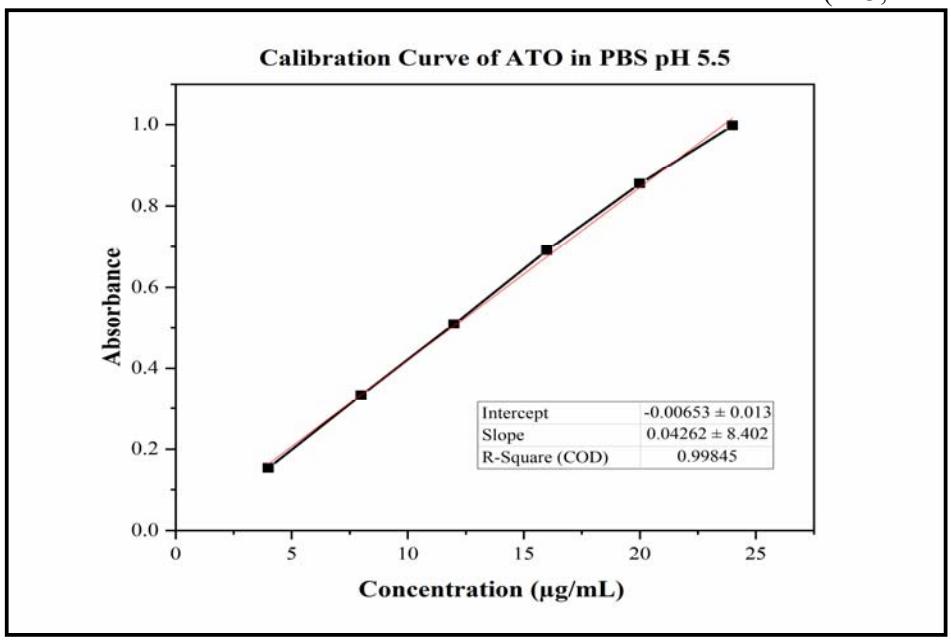

Figure-3. Calibration curve of ATO in PBS pH 5.5

D. Analytical method for estimation of Atorvastatin by HPLC:

- Instrument: 1220 LC (Agilent Technology, Germany)
- Chromatographic Conditions:
  Column: Agilent 5 HC_{18} column, (250 X 4.6mm), i.d. 5 µm,
  Flow rate: 1.0 mL/minute,
  Injection volume: 20 µL,
  Run time: 10 minutes,
  Wavelength: 244 nm,
  Temperature: ambient.
  Elution Mode (isocratic): Mobile Phase A: Mobile Phase B::30:70::0.05%Formic acid (pH 2.5 ± 0.05):ACN.

Mobile Phase Preparation:
Mobile phase A and Mobile phase B was mixed well in ratio of 30:70 and filtered through 0.45 µ PVDF membrane filter [31].

- Method for calibration curve:

Aliquots from ATO stock solution were taken in 10 mL volumetric flask and volume was make up with mobile phase to get a range from 100 ng/mL to 1000 ng/mL. The area for the range of standard solutions were measured.

Table-4. Calibration data for ATO by HPLC

Conc. (ng/mL)	Area (mAU)	% RSD
100	119181 ± 1898.75	1.59
200	230026 ± 3954.99	1.73
300	332284 ± 6368.64	1.90
400	461759 ± 7995.35	1.75
500	576913 ± 5260.35	0.90
1000	1081338 ± 8168.45	0.76

Mean SD	Slope	LOD (ng/mL)	LOQ (ng/mL)
5607.75	1071.8	2.41	7.32

(n=3, ± S.D.)

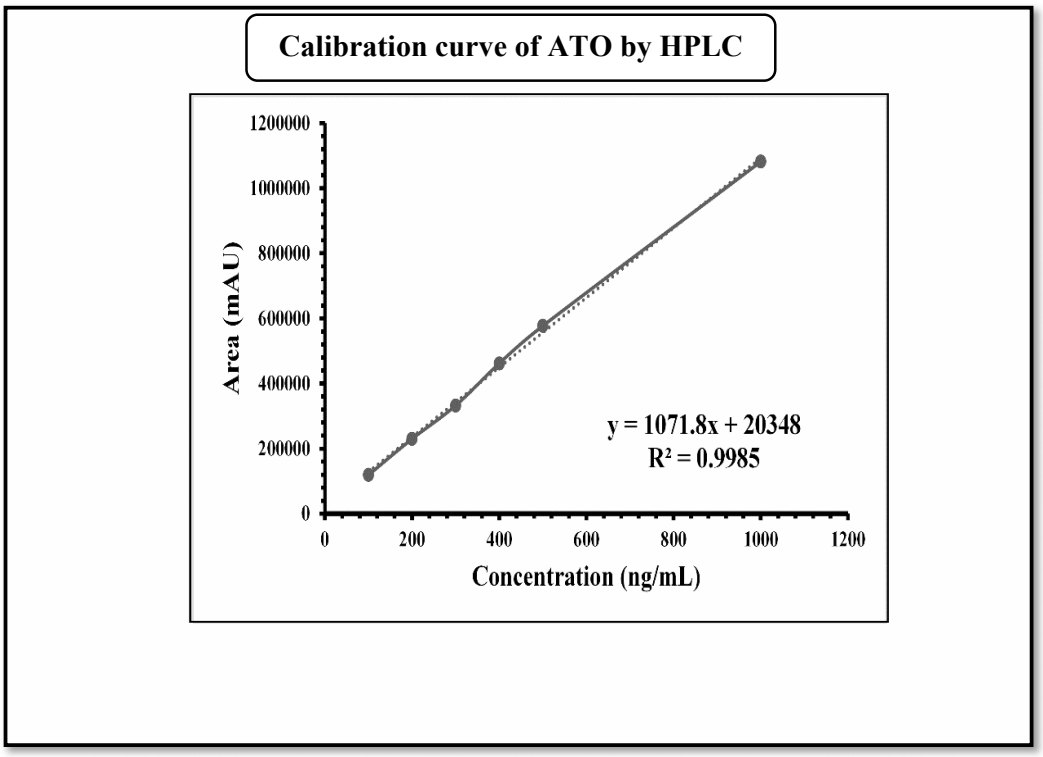

Figure-4. Calibration curve of ATO by RP-HPLC

E. Estimation of Atorvastatin in rat plasma by HPLC:

Preparation of plasma samples:

The plasma samples were prepared by spiking with aliquots of stock solution of 100 µg/mL to get concentration of 50-500 ng/mL. The protein preparation was carried out in eppendorf's (1.5ml) by addition of 0.3 mL of ACN and vertex for 2 minutes. After vertex, volume was made upto 1ml with ACN. Then samples were centrifuged at 4000 rpm for 15 min at room temperature to remove precipitated proteins. The supernatant was separated and filtered through 0.45 µ PVDF membrane filter.

- Instrument: 1220 LC (Agilent technology, Germany)

- Chromatographic Conditions:
  Column: Agilent 5 HC_{18} column, (250 X 4.6mm), i.d. 5 µm
  Flow rate: 1.0 mL/minute,
  Injection volume: 20 µL,
  Run time: 10 minutes,
  Wavelength: 244 nm,
  Temperature: ambient.
  Elution Mode (isocratic): Mobile Phase A: Mobile Phase B::30:70::0.05%Formic acid (pH 2.5 ± 0.05):ACN.

  Mobile Phase Preparation:
  Mobile phase A and Mobile phase B was mixed well in ratio of 30:70 and filtered through 0.45 µ PVDF membrane filter[31].

- Internal Standard: Clinidipine (500 ng/mL)

Table-5. Calibration Data of ATO in Plasma by HPLC

Conc. (ng/mL)	Area (mAU)	% RSD
50	50276 ± 1295.51	2.51
100	106423 ± 1932.75	1.78
200	214099 ± 6698.16	3.07
300	334034 ± 10126.96	3.02
400	454442 ± 12176.60	2.66
500	574253 ± 4666.60	0.81
1000	1034253 ± 10854.53	1.06

Mean SD	Slope	LOD (ng/mL)	LOQ (ng/mL)
7976.5	1044.1	3.99	12.10

(n=3, ± S.D.)

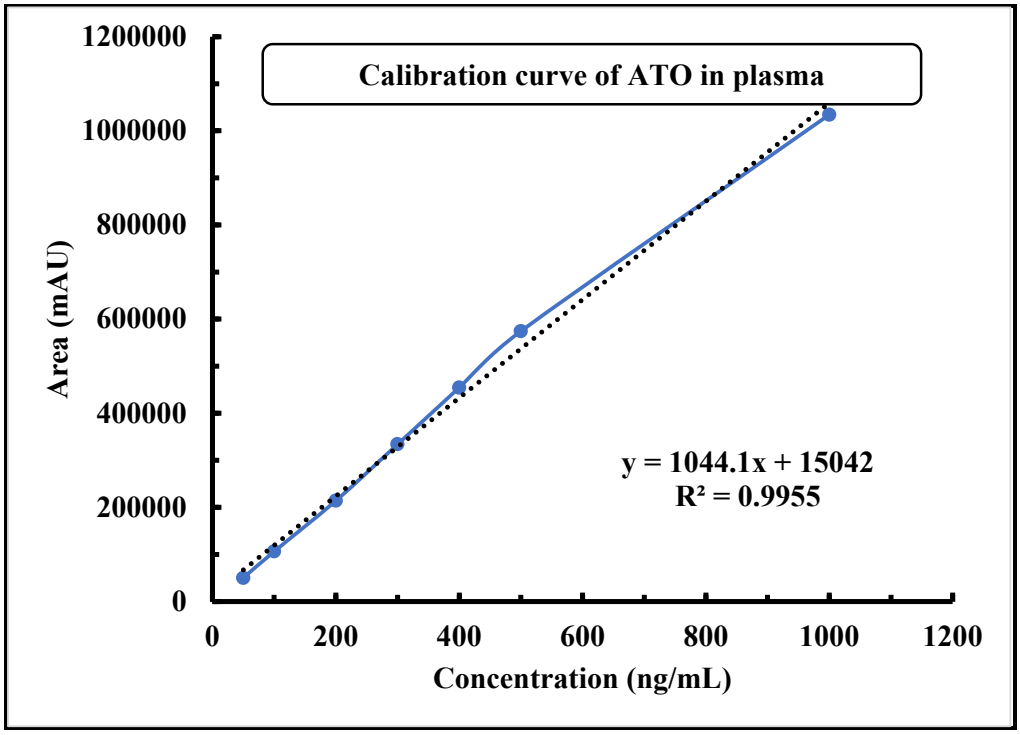

Figure-5. Calibration curve of ATO in plasma

Analytical technique for Risedronate sodium:

A. Calibration curve of Risedronate sodium in distilled water

- Procedure for calibration curve in distilled water:[32]

  Aliquots of 5 µg/mL to 50 µg/mL were prepared from RSNa stock solution (500 µg/mL) and sample was measured at 262 nm against blank (Distilled water) by UV Visible spectrophotometer.

Table-6. Calibration data of RSNa in distilled water

Conc. (µg/mL)	Absorbance ± SD (n=3)	%RSD
5	0.104 ± 0.0020	1.935
10	0.123 ± 0.0026	1.439
20	0.373 ± 0.0032	0.863
30	0.554 ± 0.0059	1.073
40	0.759 ± 0.0078	1.038
50	0.913 ± 0.0102	1.126

Mean SD	Slope	LOD	LOQ
0.0052	0.0183	0.938	2.842

(n=3, ± S.D.)

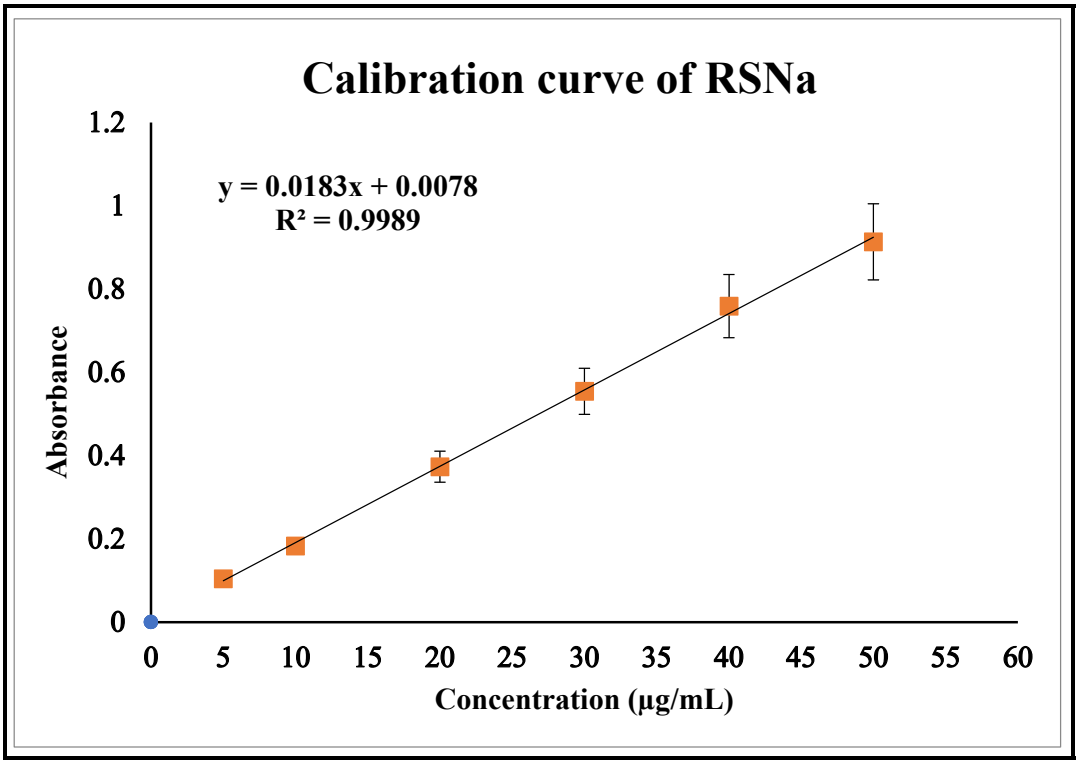

Figure-6. Calibration curve of Risedronate sodium in distilled water

B. Estimation of RSNa by RP-HPLC

- Instrument: 1220 LC (Agilent technology, Germany)
- Chromatographic Conditions:

  Column: Hypersil BDS, C_{18} column, (250 X 4.6 mm), i.d. 5 µm (Make: Thermo scientific)
  Flow rate: 1.0 mL/minute,
  Injection volume: 20 µL,
  Run time: 10 minutes,
  Wavelength: 262 nm,
  Temperature: 35°C.

- Mobile Phase (Isocratic):

  Mobile Phase A: Aqueous solution of buffer contained 11 mM sodium phosphate, 5 mM EDTA-2Na and 5 mM tetrabutylammonium hydroxide dissolved in double distilled water.
  Mobile Phase B: 100% Methanol.

  Mobile Phase Preparation:
  Mobile phase A and Mobile phase B was mixed well in ratio of 88:12 and adjusted to pH 6.75 by 1M NaOH. Then filtered through 0.45 µ PVDF membrane filter.[33]

- Method for calibration curve:

  Aliquots of 0.5 µg/mL to 6 µg/mL were prepared from RSNa stock solution (100 µg/mL) and area for the range of standard solutions were measured.

Table-7. Calibration Data of RSNa in Plasma by HPLC

Conc. (µg/mL)	Area (mAU)	% RSD
0.5	97018.33 ± 1500.47	1.54
1	242993.70 ± 4499.88	1.85
1.5	366801.30 ± 3332.81	0.90
2	463793.00 ± 5068.34	1.09
2.5	588131.70 ± 10179.91	1.76
3	680500.00 ± 5573.73	0.87
6	1214966.00 ± 9814.17	0.80

Mean SD	Slope	LOD (µg/mL)	LOQ (µg/mL)
5709.91	199222	0.094	0.287

(n=3, ± S.D.)

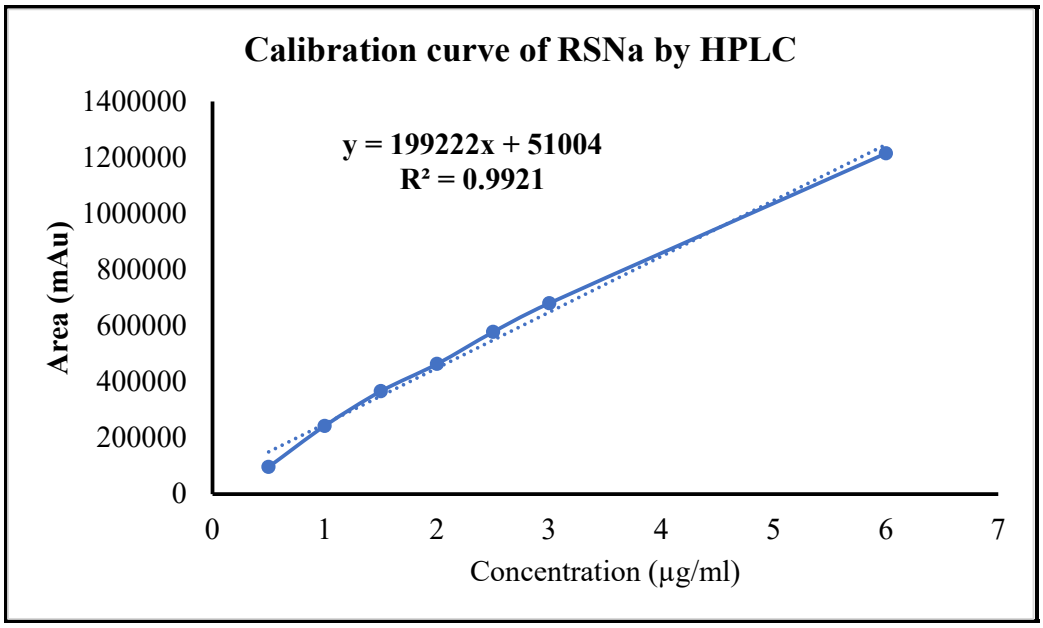

Figure-7. Calibration curve of RSNa by RP-HPLC

C. Estimation of RSNa in plasma by RP-HPLC:

- Instrument: 1220 LC (Agilent technology, Germany)
- Chromatographic Condition:

  Column: Hypersil BDS, C_{18} column, (250 X 4.6 mm), i.d. 5 µm (Make: Thermo scientific)
  Flow rate: 1.0 mL/minute,
  Injection volume: 50 µL,
  Run time: 10 minutes,
  Wavelength: 262 nm,
  Temperature: 35°C.

- Mobile Phase (Gradient):

  Buffer preparation: Aqueous solution of buffer contained 11 mM sodium phosphate, 5 mM EDTA-2Na and 5 mM tetrabutylammonium hydroxide dissolved in double distilled water adjust pH 6.75 by 1M NaOH.
  Organic Phase: 100% Methanol.
  Mobile Phase A: 88:12::Buffer: Methanol
  Mobile Phase B: 12:88:: Methanol: Buffer [33].

- Internal standard: Ascorbic acid (100 ng).

- Method for calibration curve:

  Aliquots of 400 ng/mL to 1200 ng/mL were prepared from stock solution of 5000 ng/mL. The area for the range of standard solutions were measured.

Table-8. Calibration data of RSNa in plasma by HPLC

Conc. (ng/mL)	Area (mAU)	% RSD
400	326100.33 ± 6381.31	1.96
600	459386.00 ± 8236.43	1.79
800	595609.33 ± 10255.35	1.72
1000	756474.33 ± 9532.10	1.26
1200	977420.67 ± 9600.58	0.98

Mean SD	Slope	LOD (ng/mL)	LOQ (ng/mL)
1538.06	799.86	6.37	19.28

(n=3, ± S.D.)

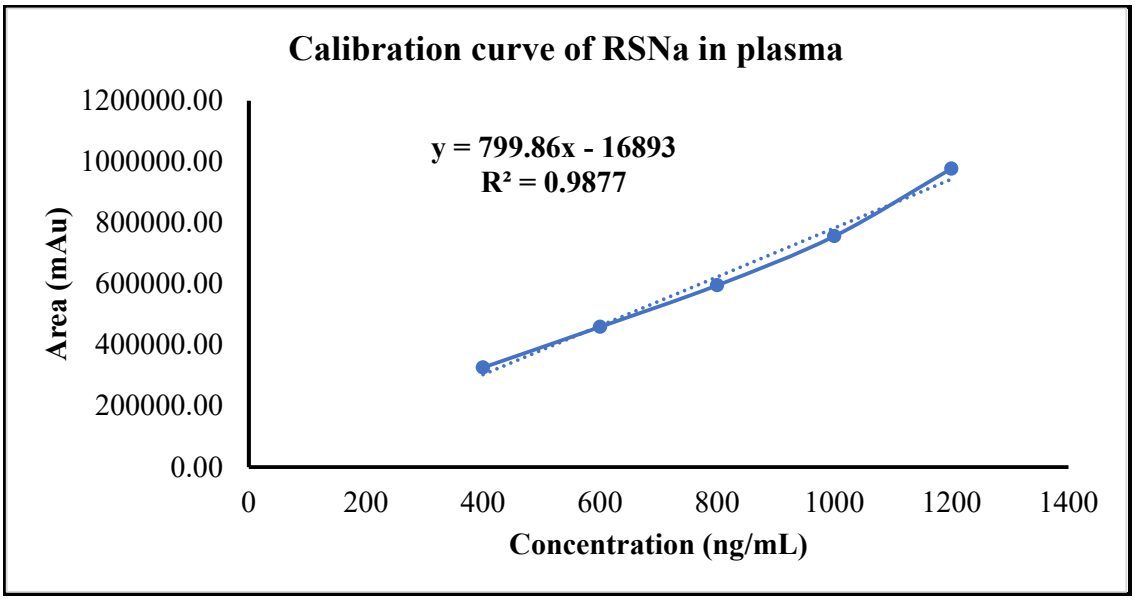

Figure-8. Calibration curve of RSNa in plasma

Preformulation studies:

A. Organoleptic properties:

The organoleptic characteristics of Atorvastatin and Risedronate are shown in table-9.

Table-9. Organoleptic characteristics of drugs

Organoleptic characteristics	Drugs	
	ATO	**RSNa**
Physical state	Solid	Solid
Appearance	Crystalline powder	Crystalline powder
Color	White	White

B. Melting Point determination:

The melting point of drugs was determined by capillary method and found to be 160-163°C and 253-258°C for ATO and RSNa respectively.

C. FTIR analysis:

The FTIR spectra of ATO and RSNa are shown in figure-9a and 9b respectively.

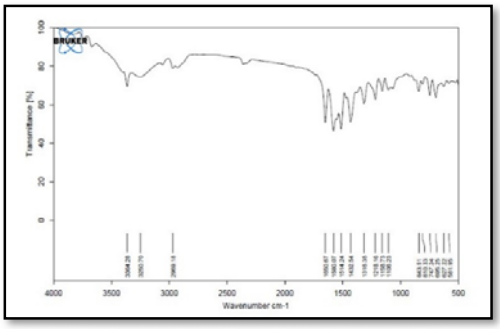

Figure-9a. FTIR spectra of ATO

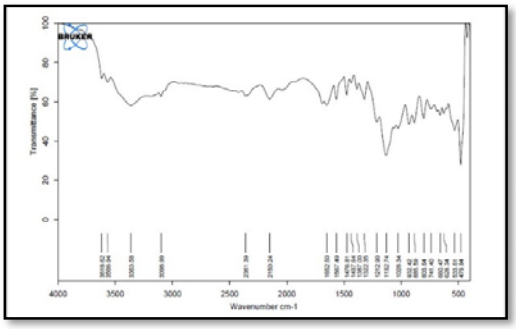

Figure-9b. FTIR spectra of RSNa

D. DSC analysis:

The thermal behaviour of ATO and RSNa was determined by Differential Scanning Calorimetry (DSC-60, Shimadzu, Japan) as shown in figure-10b and 10a respectively. The thermogram showed sharp endothermic peak at 253.2 °C and 166.19 °C for RSNa and ATO respectively.

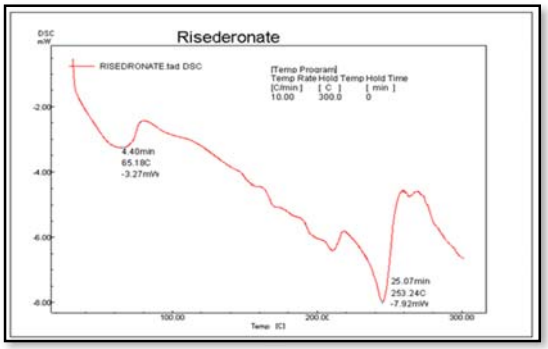

Figure-11. (a) DSC of RSNa

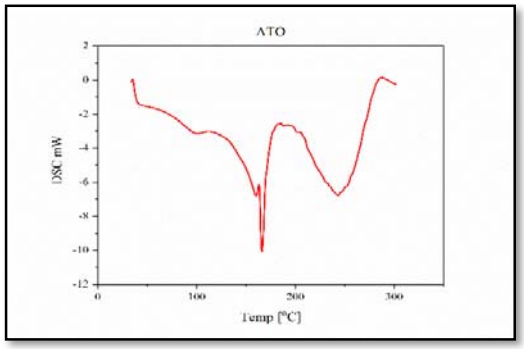

Figure-11. (b) DSC of ATO

General methods:

a. Physicochemical characteristics of nanocarriers:

The average vesicle size, polydispersity index (PDI) and zeta potential (surface charge) were analyzed by photon correlation spectroscopy using Malvern zetasizer Nano-ZS 90 (Malvern Instrument, Worcestershire, United Kingdom). All samples were analyzed in triplicate [34].

The morphology of formulated vesicles was confirmed by transmission electron microscopy (TEM). Samples were placed on carbon coated copper grid, stained with phosphotungstic acid (1%) and allowed to stand for drying [26, 35]. The residual solvents study was performed by gas chromatography (Perkin Elmer, USA) [36-38].

b. In vitro drug release study:

The release of drug from pure drug (ATO and RSNa) and drug (ATO and RSNa) loaded nanocarriers in saline PBS 7.4 as well as PBS 5.5 were performed by using dialysis bag method. Samples were withdrawn at predetermined time intervals from receptor compartment and replaced with fresh medium. The samples were analyzed spectrophotometrically. All experiments were performed in triplicate and mean value weres taken with standard deviation [13, 26, 39].

c. Ex vivo skin permeation study:

The ex vivo skin permeation of drug was performed by Franz diffusion cell using rat skin under non occlusive condition. The rat skin was sandwiched between donor filled with samples (pure drug, drug loaded nanocarriers and transdermal patches) and receptor compartment filled with PBS 7.4 at 32 ± 0.5°C under constant magnetic stirring at 100 rpm. The samples were withdrawn from receptor compartment at predetermined time intervals, filtered and analyzed [39].

d. In vitro cell line study:

1. % Cell viability study using 3T3-fibroblast cells:

The 3T3 fibroblast cells were seeded with 5×10^3 cells/well cell density in a 96 well microtiter plate using Dulbecco′s Modified Eagle′s Medium - high glucose (DMEM) supplemented with 10% Fetal Bovine Serum (FBS) and 1% antibiotic solution. This study

was done by MTT assay on the plain drug (ATO and RSNa), drug (ATO and RSNa) loaded nanocarriers, placebo of nanocarriers using PBS treated cells as control. The cells were cultured for 24 hours in an incubator with maintaining CO_2 at 5 ± 0.5 % concentration and humidified with saturated Copper sulfate solution. After 24 hrs, the media was removed, cells were washed with PBS 7.4 and replaced with complete media containing 10% FBS and 1% antibiotic. Then the cells were treated with different formulations and exposed for 12 and 24 hrs. After given exposure time, the wells were washed with PBS 7.4 and added 20 µL of MTT dye (5 mg/mL) solution in each plate. After 4 hrs, the medium in wells were replaced with 100 µL of DMSO to dissolve formazan crystals. The intensity of formazan crystals was determined using BIORAD microtiter plate reader (Biorad, California) at 570 nm. The absorbance values of cells treated with PBS were taken as 100 % cell viability and absorbances of other treated wells were compared to it. Triton X 100 and PBS 7.4 were used as negative and positive control respectively [34, 40].

2. In vitro cell permeation study:

   It was performed to determine permeability of drug across human fibroblast monolayer. Transwell® inserts of 12 mm diameter, 0.4 µm pore size (Corning, USA) with surface area of 1.12 cm^2 were used. According to protocol, Human fibroblast cells were cultured on filter support at density of 4 X 10^5 cells per well. The cells were maintained by changing media every alternate day for 21 days. The integrity of the monolayers was checked by monitoring the trans-epithelial resistance measurement using Millicell® ERS meter (Millipore, Bedford, Massachusetts, USA). After incubation, transepithelial permeation from AP to BL was carried out by placing pure drug and their formulations (drug loaded nanocarriers) on the AP side, and 1.5 mL of DMEM complete media on the BL side. Samples (200 µL) were withdrawn from BL compartments at predetermined time interval over 12 hrs. Withdrawn samples were stored at −20 °C until analyzed by HPLC. The apparent permeability coefficient (Papp in cm/s) from apical-to-basolateral was calculated as follows:

$$\text{Papp} = \frac{\text{Flux}}{\text{Initial concentration}}$$

   Where, Papp is the apparent permeability coefficient (cm/s) and initial concentration applied on the AP side (µg) [41-43].

e. Stability study of nanocarriers:

   The stability of drug (ATO and RSNa) loaded nanocarrier dispersion were studied at 2-8°C, 25±2°C/60±5% and 40±2°C/75±5% RH for 90 days with an interval of 15 days. The samples were withdrawn every 15 days and evaluated for vesicles size and % assay [39, 44-46].

Formulation of drug loaded glycerosomes:

Selection of method for preparation of glycerosomes:

Glycerosomes were prepared by thin film hydration method and reverse phase solvent evaporation method[40, 47]. ATO and RSNa were separately loaded in glycerosomes. On the basis of minimum particle size and maximum entrapment efficiency, the thin lipidic film hydration method was selected.

Preparation of glycerosomes:

Lipid and cholesterol were dissolved in organic solvent mixture of chloroform and methanol (1:1 v/v) in round bottom flask. Then organic solvent was evaporated by rotary evaporator under reduced vacuum for 30 minutes at 150 rpm to form uniform thin layer of lipid phase. The traces of organic solvents were then removed by keeping film in desiccator under reduced pressure for overnight. The prepared dried thin film was hydrated by glycerol aqueous solution for 1 hr at 150 rpm. The obtained dispersion was sonicated with optimum amplitude (2 sec ON and 2 sec OFF; optimum cycle). Then dispersion was purified by passing through Sephadex G-25 column to remove unentrapped drug and stored at 2-8°C for further study [40].

Selection of Lipid:

The lipid was selected on the basis of least particle size and high entrapment efficiency. Out of several lipids and lipidic mixtures that were screened for the preparation of glycerosomes. Lipoid S-75 was selected for the preparation of ATO as well as RSNa loaded glycerosomes.

Drug-excipient interaction study:

The drug-excipient compatibility was analysed by FTIR. The drug and mixture of excipients (lipid and cholesterol) were kept in 1:1 ratio and prepared pellets with KBr. The study revealed that no interaction was found between excipients with both drugs.

Screening of process and formulation parameters:

The process and formulation were screened and optimized on the basis of minimum particle size and maximum entrapment efficiency by one factor at a time (OFAT) approach. The various variables for preliminary screening included speed of rotation for film hydration and film formation, solvent evaporation time, hydration time, hydration volume, hydration medium, lipid:drug mole ratio, cholesterol:drug mole ratio, amplitude of sonication, sonication cycles and glycerol concentration (shown in table-10).

Table-10. Parameter screening and optimization of drug loaded glycerosomes

Variables type	**Variables**	**ATO loaded glycerosomes**		**RSN loaded glycerosomes**		**Optimized value/range**	
		Screened values				**For ATO loaded glycerosomes**	**For RSN loaded glycerosomes**
Process variables	**Solvent evaporation time for film formation (min)**	15	45	15	45	30	30
	Speed of rotation for film formation	50	150	50	150	150	150

	and hydration (RPM)						
	Hydration time (min)	30	75	30	75	60	60
	Amplitude of sonication (%)	10	70	20	70	20-60	40-60
	Cycle of sonication	10	30	10	35	15-25	15-30
Formulation variables	**Lipid:Drug (Molar ratio)**	2	6	2	9	2-6	3-6
	Cholesterol: Drug (Molar ratio)	0	1.5	0	1.5	0-1	0-1
	Glycerol concentration (% w/w)	10	40	10	40	20	20
	Hydration volume	5	15	5	10	10	5
	Hydration medium	Mili-Q water	PBS 7.4	Mili-Q water	PBS 7.4	Mili-Q water	Mili-Q water

Amongst these, the lipid:drug mole ratio, cholesterol:drug mole ratio, amplitude of sonication and sonication cycles were found to be more critical variables which showed significant effect on vesicle size and entrapment efficiency. Hence, these four factors were optimized by Definitive Screening Design (DSD) with respect to vesicle size and entrapment efficiency selected as dependent factors. The optimization was done using statistical model and desirability function, while the effect of independent variables on dependent variables was studied and analysed by software DesignExpert@V13 (Stat-Ease, Inc., USA).

Optimization of ATO loaded glycerosomes by Definitive Screening Design:

The effect of different process and formulation parameter on quality of product was analyzed by using Definitive Screening Design (DSD). The various interactive factors can be analyzed simultaneously. The influence of four factors at three level was studied with the novel design, termed as Definitive Screening Design (DSD). The variables evaluated for formulation were lipid:drug mole ratio, cholesterol:drug mole ratio, amplitude for sonication and cycles of sonication. The responses were selected as vesicle size and entrapment efficiency. For ATO loaded glycerosomes, total 13 runs, four factors, three levels DSD design were used to study the effect of independent variables on dependent variables as shown in table-11. All batches of design matrix were prepared and analyzed for vesicle size and entrapment efficiency.

Table-11. Variables selected for DSD for optimization of ATO loaded Glycerosomes.

Independent Variables		
Variables	**Low Level**	**High Level**
Lipid:Drug (Molar ratio) (A)	2	6
Cholesterol:Drug (Molar ratio) (B)	0	1
Amplitude (%) (C)	20	60
Cycles of sonication (D)	15	25
Dependent Variables		
Variables	**Goal**	**Importance**
Vesicle Size (d.nm) (Y1)	Minimize	+++
% EE (Y2)	Maximize	+++

Optimization of RSNa loaded glycerosomes by Definitive Screening Design:

The summary of independent and dependent variables with the response shown in table-12.

Table-12. variables selected for DSD for optimization of RSNa loaded Glycerosomes.

Independent Variables		
Variables	**Low Level**	**High Level**
Lipid:Drug (Molar ratio) (A)	3	6
Cholesterol:Drug (Molar ratio) (B)	0	1
Amplitude (%) (C)	40	60
Cycles of sonication (D)	15	30
Dependent Variables		
Variables	**Goal**	**Importance**
Vesicle Size (d.nm) (Y1)	Minimize	+++
% EE (Y2)	Maximize	+++

Validation of check point batch:

The check point batch obtained from design was prepared in triplicate and evaluated for vesicle size and entrapment efficiency. The check point batch for ATO loaded glycerosomes showed predicted responses of 155.5 d.nm and 89.60%, while RSNa loaded glycerosomes showed predicted responses of 148.46 d.nm and 57.44 % which were comparable with observed values. The desirability value of model for ATO loaded glycerosomes was found to be 0.969. The desirability value of model for RSNa loaded glycerosomes was found to be 0.811. The obtained

observed values were nearly related to the predicted values obtained from check point batch which is acceptable with % error. The predicted and observed values do not differ significantly at $p \leq 0.05$, hence, the results ensure the reliability of the optimization procedure.

Characterization of drug loaded glycerosomes:

a. % Entrapment Efficiency (% EE) and % Drug Loading Capacity (% DLC):

The free drug was separated by using Sephadex G-25 column for determination of entrapment efficiency. The drug loaded glycerosomal dispersion was passed through Sephadex G-25 column. Firstly, the vesicular dispersion was eluted from column and then free drug was eluted. The fraction of both entrapped and free drug sample was collected in different Eppendorf's. Then this fraction was analyzed by UV Visible spectrophotometer [48]. The % EE was calculated as follows:

$$\%EE = \frac{\text{Total drug} - \text{Free drug}}{\text{Total drug}} \times 100$$

The % drug loading capacity (% DLC) was calculated as follows:[49]

$$\%\text{DLC} = \frac{\text{Amount of drug in glycerosomes}}{Total\ solid\ contents} \times 100$$

b. Deformability Index:

Deformability index of glycerosomes was measured by extrusion method (NanoSizer™, T&T Scientific Corp., USA). The vesicular dispersion was extruded through polycarbonate filters of pore size of 50 nm. The deformability index was calculated by following equation:

$$\text{DI} = J\ (R_A|P)^2$$

Where, J is weight of dispersion collected after extrusion, R_A is average vesicle size after extrusion. P is the pore size of the extruder membrane[40, 50-52].

Physicochemical characterization of ATO loaded glycerosomes:

Table-13. Physicochemical characteristics of ATO loaded glycerosomes

Parameters	Results
Vesicle size (d.nm)	159.75 ± 5.82
PDI	0.350± 0.136
EE (%)	88.81 ± 2.33%
DLC (%)	11.00 ± 0.073
Zeta Potential (mV)	-6.08± 0.106 mV

(n=3, ± S.D.)

Physicochemical characterization of RSN loaded glycerosomes:

Table-14. Physicochemical characteristics of RSN loaded glycerosomes

Parameters	Results
Vesicle size (d.nm)	153.87 ± 4.48
PDI	0.213 ± 0.035
EE (%)	59.30 ± 1.21
DLC (%)	2.99 ± 0.055
Zeta Potential (mV)	-18.3 ± 1.00

(n=3, ± S.D.)

The morphology of formulated vesicles was confirmed by transmission electron microscopy (TEM) and it was found to be spherical in shape with particle size range within 100-200 d.nm. The residual solvents were found within limit of specification.

Impact and optimization of glycerol concentration:

The ability of glycerol to alter the stratum corneum lipid organization and hydration of stratum corneum. These characteristics of glycerol contributes to mitigate the skin barrier property and hence improve penetration of vesicles. The results of preliminary screening studies showed non-significant effects of glycerol concentration on vesicle size and entrapment efficiency. The literature survey also revealed that glycerol concentration showed significant effect on the deformability index, in vitro drug release and ex vivo skin permeation study. Hence, the glycerol concentration varies (from 10 to 30% w/w) and check the effect of glycerol concentration on in vitro drug release, deformability index and ex vivo skin permeation profile. The glycerol concentration was selected based on sustained drug release, maximum deformability index, and maximum drug skin permeation profile and compared with conventional liposomes (0% w/w glycerosomes).

1. ATO loaded glycerosomes:

   The effect of change in concentration of glycerol on physicochemical characteristics, in vitro drug release and ex vivo skin permeation were analyzed. The drug (ATO and RSNa) loaded glycerosomes were prepared by using optimized parameters obtained from design with glycerol concentration from 10 to 30% w/w and compared with drug loaded liposomes (containing 0% w/w glycerol). The effect of glycerol on physicochemical characteristics was shown in table-15 and table-16.

Table-15. Physicochemical characterization of ATO loaded glycerosomes

Glycerosomes containing glycerol concentration	Particle Size (d.nm)	PDI	Zeta Potential (mV)	% EE	% DLC	DI (%)

0% w/w	113.0± 3.35	0.403± 0.089	-3.81± 0.69	80.03± 1.19	10.03 ± 0.128	12.70 ± 1.107
10% w/w	137.3± 4.98	0.360± 0.122	-4.44± 0.63	83.98± 2.03	10.44 ± 0.095	16.21 ± 1.249
20% w/w	159.7± 5.82	0.350± 0.136	-6.08± 0.106	88.81± 2.33	11.00 ± 0.073	21.23 ± 1.659
30% w/w	161.6± 4.19	0.292± 0.048	-6.76± 0.98	90.77± 1.27	11.18 ± 0.103	31.74 ± 2.769

(n=3, ± S.D.)

*PDI- Polydispersity Index, % EE- % Entrapment efficiency, % DLC- Drug loading capacity, DI- Deformability Index.

2. RSN loaded glycerosomes:

Table-16. Physicochemical characterization of RSN loaded glycerosomes

Glycerosomes containing glycerol concentration	**Particle Size (d.nm)**	**PDI**	**Zeta Potential (mV)**	**% EE**	**% DLC**	**DI (%)**
0% w/w	97.4 ± 3.39	0.375 ± 0.071	-10.2 ± 1.27	39.71 ± 0.92	2.00 ± 0.092	11.38 ± 0.892
10% w/w	143.5 ± 4.36	0.426 ± 0.038	-16.4 ± 0.96	48.98 ± 1.59	2.44 ± 0.089	25.17 ± 2.046
20% w/w	153.8 ± 6.90	0.213 ± 0.035	-18.3 ± 1.00	59.30 ± 1.08	2.99 ± 0.055	34.81 ± 2.501
30% w/w	170.2 ± 6.74	0.246 ± 0.048	-16.3 ± 1.05	65.06 ± 1.32	3.27 ± 0.127	39.95 ± 2.858

(n=3, ± S.D.)

*PDI- Polydispersity Index, % EE- % Entrapment efficiency, % DLC- Drug loading capacity, DI- Deformability Index.

In vitro drug release study:

1. ATO loaded glycerosomes:

   The results showed that increase in concentration of glycerol in ATO loaded glycerosomes leads to reduction in the release (sustained release) of drug from glycerosomes. The release of drug was slow in PBS 5.5 as compared to PBS 7.4. The release rate of drug from ATO loaded glycerosomes in PBS 5.5 as well as PBS 7.4 was shown in figure-11 a and b respectively.

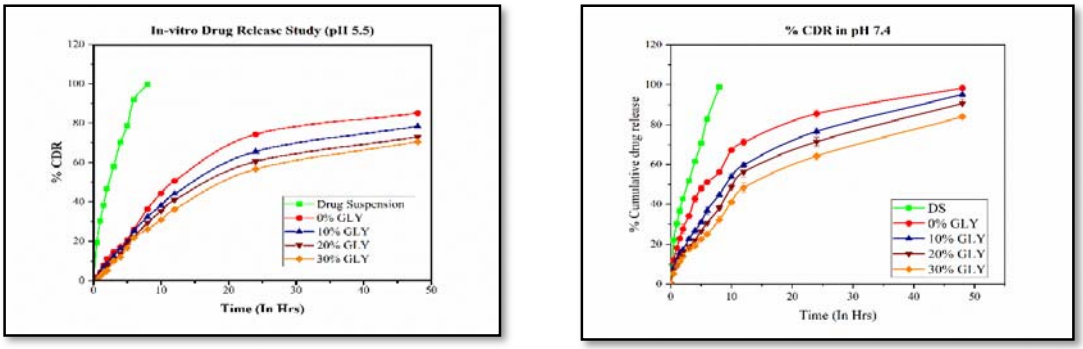

(a) (b)

Figure-11. Comparison of % cumulative drug release of ATO solution and ATO loaded glycerosomes containing different glycerol concentration (0-30% w/w) in (a) pH 5.5 and (b) pH 7.4.

2. RSN loaded glycerosomes:

The drug released within 3 hrs from pure drug; while in case of glycerosomes results showed that increase in concentration of glycerol leads to reduction (sustained release) in the drug release (shown in figure-16). On the basis of results, it was revealed that the release rate of drug was slow at PBS 5.5 (figure-12a) as compared to PBS 7.4 (figure-12a).

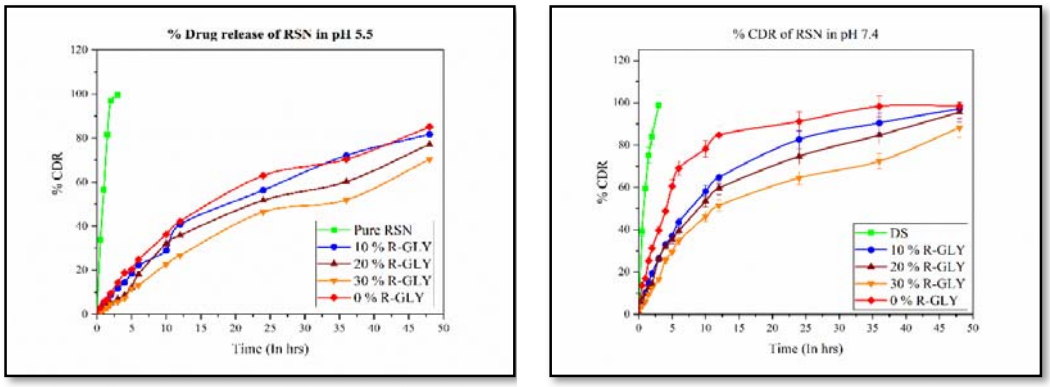

a. % CDR of RSNa in pH 5.5 b. % CDR of RSNa in pH 7.4

Figure-12. % Cumulative drug release of RSNa loaded glycerosomes

Ex vivo skin permeation study:

1. ATO loaded glycerosomes:

The results of ex vivo skin permeation are shown in figure-13. On the basis of results, it was concluded that the permeation of drug through skin increased with increase in the glycerol concentration (10 to 30% w/w) in glycerosomes as compared to plain drug and drug loaded liposomes (containing 0% w/w glycerol). On the basis of higher permeability of drug through skin, 30% w/w glycerol containing glycerosomes were selected for further in vitro cell line studies, in vivo studies. and stability study.

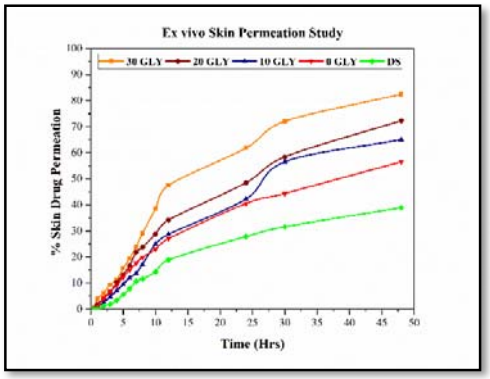

Figure-13. Ex vivo skin permeation profile of ATO loaded glycerosomes

2. RSN loaded glycerosomes:

   The results of studies revealed that increase in concentration of glycerol in glycerosomes increased the permeation of drug through skin layers. The results of skin permeation studies of RSNa loaded glycerosomes are shown in figure-14. Based on higher permeability of drug through skin, the 30% w/w glycerol containing RSNa loaded glycerosomes were selected for further in vitro cell line studies, in vivo studies, and stability study.

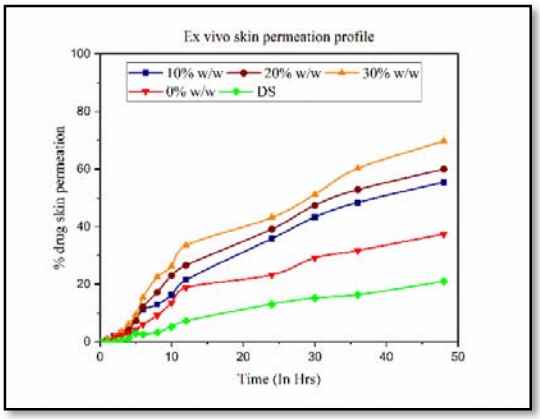

Figure-14. Ex vivo skin permeation profile of RSNa loaded glycerosomes

In vitro cell line study:

a. In vitro cell viability study:

1. For ATO Loaded Glycerosomes:

   The results of MTT assay of pure drug, ATO loaded glycerosomes and liposomes (0% w/w glycerol), placebo glycerosomes and liposomes (0% w/w glycerol) showed the cell viability more than 90% for 24 hrs. On the basis of results, it was concluded that developed glycerosomes have no potential toxic effects on fibroblast and it was found to be safe carrier for transdermal delivery.

2. For RSNa loaded glycerosomes:

   The results of cell viability studies showed that the RSNa loaded glycerosomes, RSNa loaded liposomes (0% w/w glycerol) and their placebo formulations were more viable than 90 % for

24 hrs. On the basis of results, it showed that the RSNa loaded glycerosomes will be safe and non-toxic nanocarriers for transdermal application.

b. In vitro cell permeability study:

1. For ATO Loaded Glycerosomes:

The ATO loaded glycerosomes permeated through cell layers within 4 hrs, while ATO loaded liposomes (0% w/w glycerol) permeated within 6 hrs and ATO suspension permeated through cell layers in 12 hrs. On the basis of results, it was concluded that ATO loaded glycerosomes showed more drug permeation as compared to ATO loaded liposomes (0% glycerol) and pure drug.

2. RSNa loaded glycerosomes:

In case of pure drug, about 72.19% of RSNa permeated through cell layers within 12 hrs, while RSNa-liposomes (0% w/w glycerol) permeates 96.33% and RSNa-glycerosomes permeates 97.2% of drug through cell layers in 10 hrs and 6 hrs respectively. On the basis of results, it was concluded that the RSNa loaded glycerosomes permeated more drug as compared to RSNa loaded liposomes (0% w/w glycerol) and pure drug.

Stability Study:

1. ATO loaded glycerosomes:

The results of stability studies represent no significant difference in vesicle size and % assay for ATO loaded glycerosomal dispersion and liposomes at 2-8°C and 25±2°C/60±5% RH as compared to 40±2°C/75±5% RH for 90 days. The ATO loaded glycerosomes more stable at 2-8°C and 25±2°C/60±5% RH as compared to 40±2°C/75±5% RH. On the basis of results of stability study, it was concluded that the 2-8°C and 25±2°C/60±5% RH was favourable condition for storage of ATO loaded glycerosomes for more than 90 days.

2. RSNa loaded glycerosomes:

The stability study revealed that RSNa loaded glycerosomal dispersion showed no significant difference at 2-8°C and 25±2°C/60±5% RH as compared to liposomes for 90 days. Hence, it was concluded that the 2-8°C and 25±2°C/60±5% RH was favourable condition for storage more than 90 days.

Formulation of polyelectrolyte complex nanoparticles (PECN):

Selection of polyelectrolytes:

Chitosan was complexed with different polyanions viz. chondroitin sulfate, hyaluronic acid, pectin etc. On the basis of minimum particle size and maximum entrapment efficiency, chitosan and chondroitin sulfate were selected as polycation and polyanion for preparation of PECN.

Preparation of ATO loaded PECN:

The ATO loaded PECN were prepared by polyelectrolyte self-assembled method or ionic gelation method with some modifications [53, 54]. The solution of chitosan was prepared in 1 % acetic acid and its pH was adjusted. Surfactant was added into chitosan solution and then add ATO and stirred for 15 min. Then chondroitin sulfate solution (prepared in purified distilled water) was dropwise injected into the chitosan

solution to get desired chitosan to chondroitin sulfate weight ratio with continuous stirring at 1000 RPM for 2 hrs at 25°C. The resulting nanoparticle dispersion was centrifuged at 20000 rpm for 20 min at 20°C (3 cycles) to remove unentrapped drug and NPs pellet was resuspended in purified water.

Preparation of RSNa loaded PECN:

The RSNa loaded PECN were prepared by polyelectrolyte self-assemble method or ionic gelation method with some modifications [53, 54]. The chitosan was prepared in 1 % acetic acid and its pH adjusted. The RSNa was added into chitosan solution and stirred for 15 min. Different concentration of chondroitin sulfate (prepared in purified distilled water) were added dropwise into the chitosan solution to get desired chondroitin sulfate to chitosan weight ratio with continuous stirring of 2 hrs at 25°C. The resulting solution was centrifuged at 20000 rpm for 20 min at 20°C (3 cycles) to remove free drug and NP pellet was resuspended in purified water.

Screening and optimization of process and formulation parameters:

The OFAT approach was used for the screening and optimization of drug loaded PECN. The various process parameters such as stirring time, stirring speed, rate of addition etc and formulation parameters such as concentration of chitosan, chitosan: chondroitin sulfate ratio, concentration of surfactant, pH of solution etc were screened on the basis of particle size and % EE shown in table-17.

Table-17. Parameter screening and optimization of drug loaded PECN

Variables type	**Variables**	**ATO loaded PECN**		**RSN loaded PECN**		**Optimized value/range**	
		Screened values				**For ATO loaded PECN**	**For RSN loaded PECN**
Process variables	**Rate of addition (mL/min)**	0.5	Flash addition	0.5	Flash addition	1	1
	Speed of stirring (RPM)	500	1500	500	1500	1000	1000
	Time of stirring (min)	30	150	30	150	120	120
Formulation variables	**Chitosan concentration (mg/mL)**	1	6	1	6	2-4	1-3
	Chondroitin sulfate: Chitosan ratio	2:1	1:3	2:1	1:6	1:1-1:2	1:1-1:3

Surfactant concentration (%)	0.25	1.5	-	-	1	-
pH of solution	3	7	3	7	5-7	4-6

Amongst all process and formulation parameters, Chitosan concentration, chondroitin sulfate: chitosan ratio and pH of solution were found to be most critical parameters. Hence, these three factors were optimized by Box-Behnken Design (BBD) with respect to particle size and entrapment efficiency selected as dependent factors.

Optimization of ATO loaded PECN:

For ATO loaded PECN, total 16 runs, three independent factors with three levels BBD design were used to studied the effect of independent variables on dependent variables i.e., particle size and % EE (shown in table-18).

Table-18. Variables selected for BBD for optimization of ATO loaded PECN.

Independent Variables		
Variables	**Low Level**	**High Level**
Chitosan concentration (mg/mL) (A)	2	4
Chondroitin sulfate: Chitosan ratio (B)	1:1	1:2
pH of solution (C)	5	7
Dependent Variables		
Variables	**Goal**	**Importance**
Particle Size (Y1)	Minimize	+++
% EE (Y2)	Maximize	+++

Optimization of RSNa loaded PECN:

For RSNa loaded PECN also, three factors with three levels of BBD design was used. All the batches of design matrix were prepared and analyzed for particle size and entrapment efficiency. The summary of independent and dependent variables with the goal set of response is shown in table-19.

Table-19. Variables selected for BBD for optimization of RSNa loaded PECN.

Independent Variables		
Variables	**Low Level**	**High Level**
Chitosan concentration (mg/mL) (A)	1	3
Chondroitin sulfate: Chitosan ratio (B)	1:1	1:3

pH of solution (C)	4	6
Dependent Variables		
Variables	**Goal**	**Importance**
Particle Size (Y1)	Minimize	+++
% EE (Y2)	Maximize	+++

Validation of check point batch:

The check point batch for ATO loaded PECN and RSNa loaded PECN showed predicted responses of particle size and % EE which were comparable to observed value. The desirability value of model for ATO loaded PECN was found to be 0.997. The desirability value of model for RSNa loaded PECN was found to be 0.990. Hence, the results ensured the reliability of the optimization procedure.

Physicochemical characterization of drug loaded PECN:

Differential scanning calorimetry (DSC):

Differential Scanning Calorimetry Analysis was carried out with Shimadzu DSC 60 (Japan). The samples [Drug, drug loaded PECN] were placed in aluminium pans and sealed. Thermograms were obtained by heating the samples from 20 to 300°C with a scan rate of 10°C/min with nitrogen supplied at 30 mL/min [55].

XRD study:

The X-ray diffraction analysis was analyzed to check the physical state of different components of the optimized formulation carried out by wide angle X-ray scattering ((Philips, PW 1710) with a copper anode using Sc as a detector. It was conducted at room temperature and absolute intensity was observed in the range of 10-50 versus 2θ [29, 56].

Physicochemical characterization of ATO loaded PECN:

Table-20. Physicochemical properties of ATO loaded PECN

Parameters	**Observed values**
Particle size (d.nm)	219.2 ± 5.98
PDI	0.218 ± 0.085
EE (%)	82.68 ± 2.63
DLC (%)	16.67 ± 0.098
Zeta Potential (mV)	25.41 ± 3.29

(n=3, ± S.D.)

The morphology of formulated particles was confirmed by transmission electron microscopy (TEM) and showed spherical particle size of 150-250 d.nm. The XRD study of nanoparticles revealed disappearing of intensive characteristics peak of ATO confirming encapsulation of drug into polymer matrix. The DSC graph showed absence of intensive peak of drug indicating encapsulation of drug in polymer matrix.

Physicochemical characterization of RSNa loaded PECN:

Table-21. Physicochemical properties of RSN loaded PECN

Parameters	Observed values
Particle size (d.nm)	171.6 ± 4.68
PDI	0.280 ± 0.127
EE (%)	61.13 ± 2.19
DLC (%)	13.23 ± 0.39
Zeta Potential (mV)	21.25 ± 2.18

(n=3, ± S.D.)

The morphology of formulated particles was confirmed by transmission electron microscopy (TEM) and showed spherical particles with the size range of 120-200 d.nm. The XR diffraction profile of RSN loaded PECN showed absence characteristics peak confirming encapsulation of drug into polymer matrix. The DSC graph showed absence of intensive peak of drug indicating encapsulation of drug in polymer matrix.

In vitro drug release study:

ATO loaded PECN: The % cumulative drug release from pure drug was 99.66 ± 2.26% and 98.85 ± 1.31 % in PBS 7.4 and 5.5 in 7 and 8 hrs respectively, while in case of ATO loaded PECN 62.96 ± 1.55 % and 99.61 ± 2.53 % of drug was released in PBS 5.5 and 7.4 respectively within 48 hrs (shown in figure-15a.). The release pattern of PECN showed sustained release by diffusion of drug through polymeric matrix. The ATO loaded PECN followed Higuchi model with higher regression-coefficient value in both pH 5.5 and 7.4 respectively.

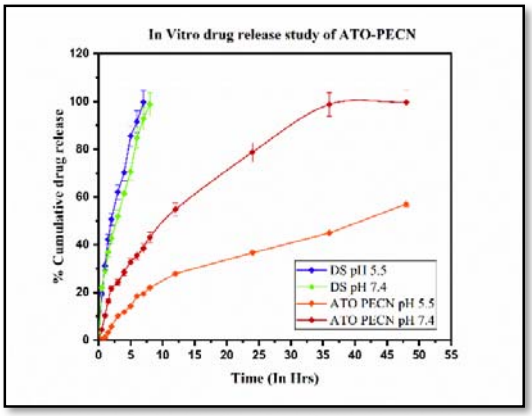

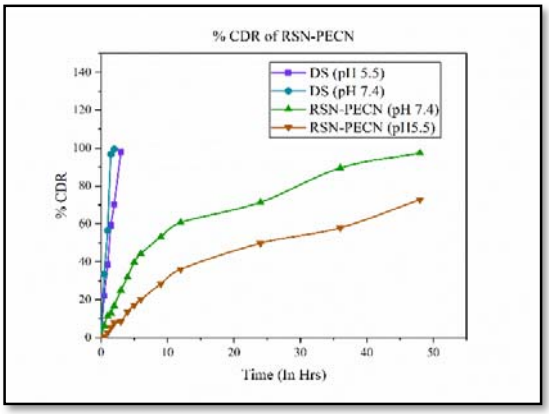

a. % drug release of ATO-PECN b. % drug release of RSN-PECN

Figure-15. % Cumulative drug release profile of PECN

RSNa loaded PECN: The % drug release from RSNa solution was found to be 97.98% and 99.50% in PBS 7.4 and PBS 5.5 within 3 hrs and 2 hrs respectively. While RSNa loaded PECN, it was found to be 97.41% and 72.79% drug release in PBS 7.4 and PBS 5.5 within 48 hrs (shown in figure-15b). The RSNa loaded PECN followed Higuchi model with higher regression-coefficient value. On the basis of results, it was concluded that the RSNa loaded PECN sustained drug release by diffusion from the matrix.

Ex vivo skin permeation study of PECN:

ATO loaded PECN: The % amount of drug permeation through skin from drug suspension after 48 hrs was found to be 35.67%, while in case of ATO loaded PECN, it was found to be 55.23% (shown in table-22). The drug permeability through skin was enhanced by 1.55 folds as compared to drug suspension.

Table-22. Ex vivo skin permeation study of PECN

Parameters / Formulation	Drug permeated through skin (%)	Drug remained on skin (%)	Drug retained in the skin (%)
ATO loaded PECN	55.23 ± 2.19	19.12 ± 3.04	26.86 ± 2.21
ATO suspension	35.67 ± 1.73	52.07 ± 4.54	10.39 ± 1.95

(n=3, ± S.D.)

RSNa loaded PECN: The % amount of RSNa permeation through skin from drug solution after 48 hrs was found to be 21.79 %, while in case of RSNa loaded PECN, it was found to be 58.47% (shown in table-23). The drug permeability through skin was enhanced by 2.68 folds as compared to drug solution.

Table-23. Ex vivo skin permeation study of PECN

Parameters / Formulation	Drug permeated through skin (%)	Drug remained on skin (%)	Drug retained in the skin (%)
RSNa loaded PECN	58.47 ± 3.10	19.50 ± 1.01	18.60 ± 2.19
RSNa Solution	21.79 ± 1.91	67.12 ± 1.45	8.96 ± 1.24

(n=3, ± S.D.)

In vitro cell viability study:

ATO loaded PECN: The results of cell viability study showed that the ATO loaded PECN and placebo PECN showed cell viability greater than 95% in 24 hrs and showed better viability than ATO suspension.

RSNa loaded PECN: The results of cell viability study showed that the RSNa loaded PECN and placebo PECN showed cell viability greater than 95% in 24 hrs and showed better viability

than RSNa solution. On the basis of cell viability results, it was concluded that the PECN was safe to use for transdermal drug delivery.

In vitro cell permeability study:

ATO loaded PECN: The results of cell permeability study showed that the ATO loaded PECN permeated drug in 8 hrs while ATO suspension permeated drugs within 12 hrs. The Papp value of ATO loaded PECN was found to be 1.05×10^{-5} cm/s, while for ATO suspension it was found to be 6.17×10^{-6} cm/s. On the basis of results, it was concluded that the ATO loaded PECN more permeated as compared to drug suspension.

RSNa loaded PECN: The RSNa loaded PECN showed 93.94 % of permeation of drug through cell layers in 10 hrs which was more permeated as compared to RSN in 12 hrs (72.19%).

Stability study:

ATO loaded PECN: The results of stability study of ATO loaded PECN showed no significant change in particle size and % assay was found at 2-8°C and 25±2°C/60±5% as compared to 40±2°C/75±5% RH over 90 days. On the basis of results, it was concluded that the ATO loaded PECN was stable at 2-8°C and 25±2°C/60±5% and was favourable condition for storage.

RSN loaded PECN: There was no significant change observed in particle size and % assay at all conditions revealed that the RSN loaded PECN was stable at 2-8°C and 25±2°C/60±5% as compared to 40±2°C/75±5% RH over 90 days.

Preparation of transdermal patch:

Method of preparation of transdermal patch:

The transdermal patch was prepared by solvent evaporation method with some modifications [57-60]. The polymer and plasticizer were added and mixed at 1000 rpm for 30 min. The mixture was then poured into petri-plate of known dimension and allowed to dry at 35 ± 2°C for 24 hrs. The patch was cut into small patch and evaluated for physicochemical characteristics.

Screening and optimization of process and formulation parameters:

The screening and optimization of process and formulation parameter for preparation of transdermal patch were done by OFAT approach. Several process parameters i.e., drying condition and time for drying and formulation parameters such as selection of polymer and its concentration, plasticizer selection and plasticizer concentration. All the batches of transdermal patches for screening and optimization were prepared as placebo. The optimization of process and formulation parameters was based on results of evaluation parameters viz. appearance, thickness, folding endurance, tensile strength, % moisture uptake and moisture loss. After optimization of transdermal patch, incorporation of drug loaded nanocarriers was done.

On the basis of results of evaluation parameters, HPMC K4M was selected as polymer with optimum concentration of 2% w/v, while polyethylene glycol-400 was selected as plasticizer with optimum concentration of 5% v/v. The prepared transdermal patches were dried at 40±5°C in vacuum oven which was considered as optimum drying condition for preparation of desirable transdermal patch.

Physical Attributes:

The transdermal patches were assessed for morphological parameters like color, clarity, surface texture and homogeneity. The weight variation [60], thickness [61], folding endurance [62] and flatness of patches [62] were measured [63].

Drug content:

The patch of size of 2 X 2 cm was cut from three different places and dissolved in suitable solvent. The appropriate dilution was made and analyzed by UV spectrophotometer against blank (UV -1900, Shimadzu, Japan) [62].

Percentage moisture uptake and moisture content:

The prepared patches were cut (2 X 2 cm) and accurately weighed. Then, these patches kept in desiccator containing calcium chloride at room temperature for 24 hrs. After 24 hrs, each patch was reweighed separately and until a weight of patch gets constant. The moisture content of patch was calculated by changing in patch weight over initial patch weight [63].

The moisture uptake capacities of patch were measured at 84 % RH. The patches were cut (2 X 2 cm) and accurately weighed at predetermined time interval until the patch weights get constant. The moisture absorption capacity of patches was determined by change in patch weight over initial weight. The moisture uptake and moisture content were calculated by following equation: [63]

$$Moisture\ Uptake\ (\%) = \frac{Final\ weight - Initial\ weight}{Initial\ weight} \times 100$$

$$Moisture\ Content\ (\%) = \frac{Initial\ weight - Final\ weight}{Final\ weight} \times 100$$

Tensile strength:

The tensile strength of patch was determined by digital tensiometer (Brookfield texture analyzer; Brookfield, IL, USA) by clamping the patch of specific dimension (2 X 2 cm). The patch was elongated by instrument till patch deformed. The force and distance travelled was calculated by instruments and graph was generated [60].

$$Tensile\ strength = \frac{Breaking\ force\ (g)}{Cross\ sectional\ area\ of\ film\ (cm^2)}$$

Incorporation of drug loaded glycerosomes:

HPMC K4M as a polymer and Polyethylene glycol-400 as a plasticizer was added in drug loaded glycerosomal dispersion and mixed at 1000 rpm for 15 min. The mixture was then poured into a petri-plate with known dimensions and allowed to dry for 24 hours at 35±2°C. After drying, the formed patch was carefully removed. The patch was cut into small patches and evaluated for physicochemical characteristics [57-60].

Incorporation of ATO loaded Glycerosomes into transdermal patch:

Table-24. Physicochemical characteristics of ATO-glycerosomal optimized transdermal patches

PARAMETERS	VALUES		
	0 % w/w*	**30 % w/w***	**ATO Loaded Patch**
Appearance	Clear and Transparent	Clear and Transparent	Clear and Transparent
Thickness (mm)	0.32 ± 0.005	0.40 ± 0.011	0.34 ± 0.015
Weight (mg)	152.6 ± 1.65	155.3 ± 1.98	140.2 ± 1.74
% Moisture content	2.62 ± 0.97	1.58 ± 0.41	1.95 ± 0.72s
% Moisture uptake	1.13 ± 0.22	1.95 ± 0.43	1.25 ± 0.55
Tensile Strength (g/cm^2)	741.58 ± 15.93	1084.41 ± 19.06	702.00 ± 8.28
% Drug content	98.25 ± 1.25	99.12 ± 2.22	98.96 ± 2.03
Folding endurance	391 ± 4.72	409 ± 3.78	401 ± 4.93

* % w/w glycerol containing ATO loaded glycerosomal transdermal patch. (n=3, ± S.D.)

Incorporation of RSN loaded Glycerosomes into transdermal patch:

Table-25. Physicochemical characteristics of RSNa-glycerosomal transdermal patches

PARAMETERS	VALUES		
	0 % w/w*	**30 % w/w***	**RSNa Loaded Patch**
Appearance	Clear and Transparent	Clear and Transparent	Clear and Transparent
Thickness (mm)	0.40 ± 0.005	0.42 ± 0.011	0.38 ± 0.015
Weight (mg)	154.8 ± 1.05	151.9 ± 0.95	139.2 ± 1.27
% Moisture content	2.41 ± 0.35	1.48 ± 0.45	1.74 ± 0.55
% Moisture uptake	1.89 ± 0.40	2.69 ± 0.55	1.21 ± 0.67
Tensile Strength (g/cm^2)	919.91 ± 16.23	1674.0 ± 11.53	878.08 ± 17.20
% Drug content	99.15 ± 1.52	99.03 ± 0.78	99.84 ± 1.42
Folding endurance	400 ± 2	415 ± 2	388 ± 4

*% w/w glycerol containing RSNa loaded glycerosomal transdermal patch. (n=3, ± S.D.)

Incorporation of drug loaded PECN:

Selection and optimization of penetration enhancers:

The polyelectrolyte complex nanoparticles showed slower diffusion of drug through skin which was studied earlier in ex vivo skin permeation study. The addition of a penetration enhancer (PE) might help to improve the ability of drug penetration through skin layers. Hence, the penetration enhancers were required in the preparation of the transdermal patch containing drug-loaded PECN. The penetration enhancers in drug loaded PECN incorporated transdermal patch was done by using different penetration enhancers like olive oil, glycerol, oleic acid, IPM and propylene glycol. The drug loaded PECN with permeation enhancer incorporated transdermal patch were subjected for ex vivo skin permeation study by Franz diffusion cell using rat skin. The amount of drug permeated through skin in 24 hrs was calculated and selection of permeation enhancers and its concentration was selected.

ATO loaded PECN: The results of selection and optimization of penetration enhancers showed that 0.2% glycerol (as penetration enhancer) permeated more amount of ATO i.e., 52.26 ± 2.36% through skin within 24 hrs as compared to other penetration enhancers.

RSNa loaded PECN: The results showed that amongst all penetration enhancers, glycerol permeated 47.11% of RSN through skin within 24 hrs which was higher than other penetration enhancers at 0.2 % of concentration. Hence, 0.2% glycerol was selected as penetration enhancer with 0.2% w/w concentration for preparation of PECN incorporated transdermal patch.

Preparation of PECN incorporated transdermal patch:

2% w/v HPMC K4M as a polymer, 5%w/v Polyethylene glycol-400 as a plasticizer with 0.2% w/v permeation enhancer (glycerol) was added in dispersion of drug (ATO or RSNa) loaded PECN and mixed at 1000 rpm for 15 min. The mixture was then poured into a petri-plate with known dimensions and allowed to dry for 24 hours at 35±2°C. After drying, the formed patch was carefully removed and cut into small pieces [57-60].

Physicochemical characteristics:

ATO-PECN loaded transdermal patch:

The physicochemical characteristics of ATO-PECN incorporated transdermal patch are shown in table-26.

Table-26. Physicochemical characteristics of ATO-PECN transdermal patches

PARAMETERS	**VALUES**		
	Without penetration enhancer*	**With Penetration enhancer***	**ATO Loaded transdermal Patch**
Appearance	Clear and Transparent	Clear and Transparent	Clear and Transparent
Thickness (mm)	0.41 ± 0.005	0.44 ± 0.010	0.39 ± 0.005
Weight (mg)	150.2 ± 2.07	162.3 ± 1.81	144.6 ± 1.30

% Moisture content	3.36 ± 0.35	2.94 ± 0.33	1.84 ± 0.50
% Moisture uptake	1.20 ± 0.85	1.63 ± 0.61	1.58 ± 0.23
Tensile Strength (g/cm^2)	820.75 ± 11.67	1162.25 ± 19.55	766.25 ± 8.28
% Drug content	99.11 ± 1.08	98.26 ± 0.52	99.39 ± 0.66
Folding endurance	327 ± 3.61	368 ± 4.04	399 ± 3.51

*ATO loaded PECN (n=3, ± S.D.)

RSN loaded PECN incorporated transdermal patch:

The physicochemical characteristics of RSNa-PECN incorporated transdermal patch are shown in table-27.

Table-27. Physicochemical characteristics of RSN-PECN transdermal patches

PARAMETERS	**VALUES**		
	Without penetration enhancer*	**With Penetration enhancer***	**RSN Loaded transdermal Patch**
Appearance	Clear and Transparent	Clear and Transparent	Clear and Transparent
Thickness (mm)	0.39 ± 0.004	0.43 ± 0.012	0.38 ± 0.004
Weight (mg)	153.3 ± 0.43	164.9 ± 0.46	148.3 ± 0.37
% Moisture content	3.45 ± 0.27	2.07 ± 0.13	1.82 ± 0.25
% Moisture uptake	1.53 ± 0.24	1.81 ± 0.28	1.87 ± 0.13
Tensile Strength (g/cm^2)	928.75 ± 20.30	1113.16 ± 13.50	813.08 ± 17.20
% Drug content	98.28 ± 0.5	98.65 ± 0.8	99.72 ± 1.0
Folding endurance	350 ± 3.68	372 ± 2.05	380 ± 2.49

*RSNa loaded PECN (n=3, ± S.D.)

Ex vivo skin permeation study:

Results and discussion:

ATO-glycerosomal transdermal patch: The results showed (shown in table-28) that 30% w/w glycerosomal transdermal patches enhanced the permeation of ATO through skin layers as compared to 0% w/w glycerosomes (liposomes) and drug loaded patch.

Table-28. Ex vivo skin permeation study of ATO loaded glycerosomal patch

Parameters / Formulation	Drug permeated through skin (%)	Drug remained on skin (%)	Drug retained in the skin (%)
0% w/w*	63.07 ± 1.52	23.87 ± 1.19	9.33 ± 0.69
30% w/w*	82.61 ± 3.29	8.32 ± 1.07	4.16 ± 1.11
ATO Suspension	52.06 ± 1.92	41.91 ± 3.55	9.36 ± 1.52

*% w/w glycerol containing ATO loaded glycerosomal transdermal patch (n=3, ± S.D.)

RSNa-glycerosomal transdermal patch: The results of ex vivo study showed (shown in table-29) that the 30% w/w RSNa loaded glycerosomes enhanced permeation of drug through skin as compared to liposomes (0% w/w glycerosomes) and RSNa loaded transdermal patch.

Table-29. Ex vivo skin permeation study of RSNa loaded glycerosomal patch

Parameters / Formulation	Drug permeated through skin (%)	Drug remained on skin (%)	Drug retained in the skin (%)
0% w/w*	48.37 ± 2.69	28.28 ± 1.49	21.62 ± 1.77
30% w/w*	87.12 ± 3.04	5.88 ± 1.20	8.37 ± 1.69
RSN Solution	34.71 ± 2.97	49.01 ± 1.82	14.24 ± 1.39

*% w/w glycerol containing RSNa loaded glycerosomal transdermal patch (n=3, ± S.D.)

ATO-PECN incorporated transdermal patch: The results of ex vivo skin permeation showed that more amount of ATO was permeated through skin by PECN transdermal patch containing penetration enhancer (glycerol) as compared to ATO loaded patch and ATO loaded PECN without penetration enhancer. The % amount of drug permeated through skin from ATO loaded transdermal patch and ATO loaded PECN without glycerol transdermal patch was found to be 48.73 ± 1.63 % and 65.02 ± 2.56 % respectively, while 83.22 ± 3.67% of drug permeated through skin from ATO loaded PECN with glycerol transdermal patch (shown in table-30).

Table-30. Ex vivo skin permeation study of ATO-PECN transdermal patch

Parameters / Formulation	Drug permeated through skin (%)	Drug remained on skin (%)	Drug retained in the skin (%)
Without PE*	65.02 ± 2.56	20.15 ± 1.58	8.42 ± 1.16
With PE*	83.22 ± 3.67	6.30 ± 0.98	9.34 ± 1.08
ATO loaded transdermal patch	48.73 ± 1.63	39.85 ± 2.24	8.30 ± 1.01

*ATO-PECN transdermal patch (n=3, ± S.D.)

RSNa-PECN incorporated transdermal patch: The results showed that 81.26 ± 2.57% of RSNa permeated through skin within 72 hrs from RSNa-PECN loaded transdermal patch containing glycerol. 73.83 ± 3.19% and 35.46 ± 1.71% of RSN permeated through skin within 72 hrs from RSNa-PECN loaded transdermal patch without glycerol and RSNa loaded transdermal patch (shown in table-31).

Table-31. Ex vivo skin permeation study of RSNa-PECN transdermal patch

Parameters / Formulation	Drug permeated through skin (%)	Drug remain on skin (%)	Drug retained in the skin (%)
Without PE*	73.83 ± 3.19	13.66 ± 0.91	12.60 ± 1.12
With PE*	81.26 ± 2.57	12.59 ± 1.22	4.77 ± 0.95
RSN loaded transdermal patch	35.46 ± 1.71	45.86 ± 1.68	17.15 ± 1.40

*RSNa-PECN transdermal patch (n=3, ± S.D.)

Evaluation of skin structure after treatment of drug loaded nanocarriers incorporated transdermal patch**:**

The effect of transdermal patch (containing drug loaded nanocarriers) on rat skin structure integrity after application was performed by FTIR. The patch was applied on rat skin and sandwiched between donor-receptor compartment in Franz diffusion cell. After treatment of 24 hrs, the skin was washed with PBS, dried, and subjected to FTIR analysis. The spectra of treated skin were compared with untreated skin which was used as control [64-66]. The study was performed on rat skin by treating with ATO loaded glycerosomal patch, RSNa loaded glycerosomal patch, ATO-PECN incorporated patch and RSNa-PECN incorporated patch in comparison with normal (non-treated) skin.

The results of FTIR study revealed that there was no change in characteristics peaks of treated skin as compared to non-treated skin. On the basis of results, it was concluded that there was no significant effect of nanocarriers incorporated transdermal patch found on the integrity of skin.

Ex vivo skin permeation analysis by using fluorescence microscopy:

The distribution of formulation through different skin layers was analysed by fluorescence microscopy. The dye loaded nanocarriers were prepared by methods used in preparation of glycerosomes and PECN using 1 % of dye incorporated into transdermal patch. Using a Franz diffusion cell, dye-loaded nanocarriers incorporated into transdermal patches were applied to rat skin. After treatment for 24 hrs, the skin was washed and a transectional section of skin was taken using a cryo-sectional cutter. The images of sectional area of skin were observed in fluorescence microscope and compared with untreated skin specimen [67-69].

The results of fluorescence microscopy showed that the drug loaded nanocarriers penetrated through deep skin layers. The fluorescence microscopy of drug loaded nanocarriers treated skin compared with untreated skin confirmed efficient delivery of nanocarriers through the skin.

Stability study:

The storage stability of transdermal patch (containing drug loaded nanocarriers) was carried out at different temperatures viz. 2-8°C, 25±2°C/60±5% RH and 40±2°C/75±5% RH for 60

days. Samples were monitored by analysing for drug content, tensile strength, weight, and moisture content over 90 days in interval of 30 days [70].

The results of stability study revealed that the transdermal patch appeared clear, smooth, and transparent in nature after more than 90 days of stability. On the basis of results, it was concluded that there was no significant difference found in folding endurance, % drug content, weight and thickness at 2-8°C and 25±2°C/60±5% RH conditions over for more than 90 days. The results of stability study revealed that the drug loaded nanocarriers incorporated transdermal patch was stable at 2-8°C and 25±2°C/60±5% RH for more than 90 days.

Ongoing work:

1. In vivo pharmacokinetic study
2. In vivo pharmacodynamic study

References:

1. Kendler, D.L., et al., *Osteoporosis management in hematologic stem cell transplant recipients: Executive summary.* Journal of Bone Oncology, 2021. **28**: p. 100361.
2. Tu, K.N., et al., *Osteoporosis: a review of treatment options.* Pharmacy and Therapeutics, 2018. **43**(2): p. 92.
3. Oden, A., et al., *Burden of high fracture probability worldwide: secular increases 2010–2040.* Osteoporosis International, 2015. **26**(9): p. 2243-2248.
4. Sözen, T., L. Özışık, and N.Ç. Başaran, *An overview and management of osteoporosis.* European journal of rheumatology, 2017. **4**(1): p. 46.
5. Drake, M.T., B.L. Clarke, and E.M. Lewiecki, *The pathophysiology and treatment of osteoporosis.* Clinical therapeutics, 2015. **37**(8): p. 1837-1850.
6. Sandhu, S.K. and G. Hampson, *The pathogenesis, diagnosis, investigation and management of osteoporosis.* Journal of clinical pathology, 2011. **64**(12): p. 1042-1050.
7. CHILCOTT, W., *FDA Drug Approvals.*
8. Fazil, M., et al., *Biodegradable intranasal nanoparticulate drug delivery system of risedronate sodium for osteoporosis.* Drug delivery, 2016. **23**(7): p. 2428-2438.
9. Nam, S.H., et al., *Topically administered Risedronate shows powerful anti-osteoporosis effect in ovariectomized mouse model.* Bone, 2012. **50**(1): p. 149-155.
10. Sahana, H., et al., *Improvement in bone properties by using risedronate adsorbed hydroxyapatite novel nanoparticle based formulation in a rat model of osteoporosis.* Journal of biomedical nanotechnology, 2013. **9**(2): p. 193-201.
11. Khan, A.-W. and A. Khan, *Anabolic agents: a new chapter in the management of osteoporosis.* Journal of Obstetrics and Gynaecology Canada, 2006. **28**(2): p. 136-141.
12. An, T., et al., *Efficacy of statins for osteoporosis: a systematic review and meta-analysis.* Osteoporosis International, 2017. **28**(1): p. 47-57.
13. Xie, Y., et al., *Atorvastatin-loaded micelles with bone-targeted ligand for the treatment of osteoporosis.* Drug Delivery, 2017. **24**(1): p. 1067-1076.
14. El-Nabarawi, N., M. El-Wakd, and M. Salem, *Atorvastatin, a double weapon in osteoporosis treatment: an experimental and clinical study.* Drug design, development and therapy, 2017. **11**: p. 1383.
15. Keleb, E., et al., *Transdermal drug delivery system-design and evaluation.* International journal of advances in pharmaceutical sciences, 2010. **1**(3).
16. Brown, M.B., et al., *Dermal and transdermal drug delivery systems: current and future prospects.* Drug delivery, 2006. **13**(3): p. 175-187.
17. Ramadon, D., et al., *Enhancement strategies for transdermal drug delivery systems: Current trends and applications.* Drug Delivery and Translational Research, 2022. **12**(4): p. 758-791.
18. Patel, D., et al., *Transdermal drug delivery system: a review.* The pharma innovation, 2012. **1**(4, Part A): p. 66.
19. Escobar-Chávez, J.J., et al., *Nanocarriers for transdermal drug delivery.* Research and Reports in Transdermal Drug Delivery, 2012. **1**: p. 3.
20. Essa, E.A., M.C. Bonner, and B.W. Barry, *Human skin sandwich for assessing shunt route penetration during passive and iontophoretic drug and liposome delivery.* Journal of pharmacy and pharmacology, 2002. **54**(11): p. 1481-1490.
21. Das Kurmi, B., et al., *Transdermal drug delivery: opportunities and challenges for controlled delivery of therapeutic agents using nanocarriers.* Current drug metabolism, 2017. **18**(5): p. 481-495.
22. Kumar, G.P. and P.R. Rao, *Ultra deformable niosomes for improved transdermal drug delivery: The future scenario.* Asian Journal of Pharmaceutical Sciences, 2012. **7**(1).
23. ud Din, F., et al., *Effective use of nanocarriers as drug delivery systems for the treatment of selected tumors.* International journal of nanomedicine, 2017. **12**: p. 7291.
24. Peer, D., et al., *Nanocarriers as an emerging platform for cancer therapy.* Nano-Enabled Medical Applications, 2020: p. 61-91.

25. Manca, M.L., et al., *Glycerosomes: A new tool for effective dermal and transdermal drug delivery.* 2013. **455**(1-2): p. 66-74.
26. Salem, H.F., et al., *Formulation design and optimization of novel soft glycerosomes for enhanced topical delivery of celecoxib and cupferron by Box–Behnken statistical design.* Drug development and industrial pharmacy, 2018. **44**(11): p. 1871-1884.
27. Meka, V.S., et al., *A comprehensive review on polyelectrolyte complexes.* Drug discovery today, 2017. **22**(11): p. 1697-1706.
28. Sharma, S., K.L. Swetha, and A. Roy, *Chitosan-Chondroitin sulfate based polyelectrolyte complex for effective management of chronic wounds.* International journal of biological macromolecules, 2019. **132**: p. 97-108.
29. Talib, S., et al., *Chitosan-chondroitin based artemether loaded nanoparticles for transdermal drug delivery system.* Journal of Drug Delivery Science and Technology, 2021. **61**: p. 102281.
30. Yilmaz, B. and S. Kaban, *UV and First Derivative Spectrophotometric Methods for the Estimation of Atorvastatin in Pharmaceutical Preparations.* Journal of Advanced Pharmacy Research, 2018. **2**(2): p. 89-94.
31. AlKhani, M., A. Al-Laham, and M.A. Al-Mardini, *Simultaneous and precise HPLC method for quantification of atorvastatin in rat plasma and intestinal perfusion solution.* Int J Pharm Sci Rev Res, 2016. **38**(2): p. 70-4.
32. Swami, A.S., S.A. Pishawikar, and H.N. More, *Development and validation of stability indicating uv spectrophotometric method for the estimation of sodium risedronate.* International journal of pharmacy and pharmaceutical sciences, 2012. **4**(3): p. 4.
33. Jia, H.-J., W. Li, and K. Zhao, *Determination of risedronate in rat plasma samples by ion-pair high-performance liquid chromatography with UV detector.* Analytica Chimica Acta, 2006. **562**(2): p. 171-175.
34. Manca, M.L., et al., *Glycerosomes: Use of hydrogenated soy phosphatidylcholine mixture and its effect on vesicle features and diclofenac skin penetration.* International journal of pharmaceutics, 2016. **511**(1): p. 198-204.
35. Rani, D., et al., *Formulation development and in-vitro evaluation of minoxidil bearing glycerosomes.* Am. J. Biomed. Res, 2016. **4**: p. 27-37.
36. Han, E.-J., A.-H. Chung, and I.-J. Oh, *Analysis of residual solvents in poly (lactide-co-glycolide) nanoparticles.* Journal of Pharmaceutical Investigation, 2012. **42**(5): p. 251-256.
37. Yang, Y., X.Y. Xie, and X.G. Mei, *Preparation and in vitro evaluation of thienorphine-loaded PLGA nanoparticles.* Drug delivery, 2016. **23**(3): p. 777-783.
38. Grodowska, K. and A. Parczewski, *Analytical methods for residual solvents determination in pharmaceutical products.* Acta Poloniae Pharmaceutica. Drug Research, 2010. **67**(1).
39. Mahmoud, M.O., et al., *Transdermal delivery of atorvastatin calcium from novel nanovesicular systems using polyethylene glycol fatty acid esters: ameliorated effect without liver toxicity in poloxamer 407-induced hyperlipidemic rats.* Journal of controlled release, 2017. **254**: p. 10-22.
40. Manca, M.L., et al., *Glycerosomes: A new tool for effective dermal and transdermal drug delivery.* International journal of pharmaceutics, 2013. **455**(1-2): p. 66-74.
41. Shah, P., et al., *In vitro assessment of acyclovir permeation across cell monolayers in the presence of absorption enhancers.* Drug development and industrial pharmacy, 2008. **34**(3): p. 279-288.
42. Chen, S., R. Einspanier, and J. Schoen, *Transepithelial electrical resistance (TEER): a functional parameter to monitor the quality of oviduct epithelial cells cultured on filter supports.* Histochemistry and cell biology, 2015. **144**(5): p. 509-515.
43. Poenar, D.P., et al., *Low-cost method and biochip for measuring the trans-epithelial electrical resistance (TEER) of esophageal epithelium.* Materials, 2020. **13**(10): p. 2354.
44. Sharma, D., et al., *Formulation and optimization of polymeric nanoparticles for intranasal delivery of lorazepam using Box-Behnken design: in vitro and in vivo evaluation.* BioMed research international, 2014. **2014**.

45. Manca, M.L., et al., *Glycerosomes: Investigation of role of 1, 2-dimyristoyl-sn-glycero-3-phosphatidycholine (DMPC) on the assembling and skin delivery performances.* International Journal of Pharmaceutics, 2017. **532**(1): p. 401-407.
46. Rani, D., et al., *Formulation, design and optimization of glycerosomes for topical delivery of minoxidil.* Res. J. Pharmacol. Technol, 2021. **14**: p. 2367-2374.
47. Zhang, K., et al., *Essential oil-mediated glycerosomes increase transdermal paeoniflorin delivery: Optimization, characterization, and evaluation in vitro and in vivo.* International journal of nanomedicine, 2017. **12**: p. 3521.
48. Zhang, K., et al., *Preparation, characterization, and in vivo pharmacokinetics of nanostructured lipid carriers loaded with oleanolic acid and gentiopicrin.* International journal of nanomedicine, 2013. **8**: p. 3227.
49. Duangjit, S., et al., *Characterization and in vitro skin permeation of meloxicam-loaded liposomes versus transfersomes.* Journal of drug delivery, 2011. **2011**.
50. Naguib, M.J., et al., *Investigating the potential of utilizing glycerosomes as a novel vesicular platform for enhancing intranasal delivery of lacidipine.* International Journal of Pharmaceutics, 2020. **582**: p. 119302.
51. Fahmy, A.M., et al., *Statistical optimization of hyaluronic acid enriched ultradeformable elastosomes for ocular delivery of voriconazole via Box-Behnken design: in vitro characterization and in vivo evaluation.* Drug delivery, 2021. **28**(1): p. 77-86.
52. Molinaro, R., et al., *Development and in vivo evaluation of multidrug ultradeformable vesicles for the treatment of skin inflammation.* Pharmaceutics, 2019. **11**(12): p. 644.
53. Jardim, K.V., et al., *Physico-chemical characterization and cytotoxicity evaluation of curcumin loaded in chitosan/chondroitin sulfate nanoparticles.* Materials science and engineering: c, 2015. **56**: p. 294-304.
54. Rezazadeh, M., et al., *Incorporation of rosuvastatin-loaded chitosan/chondroitin sulfate nanoparticles into a thermosensitive hydrogel for bone tissue engineering: preparation, characterization, and cellular behavior.* Pharmaceutical Development and Technology, 2019. **24**(3): p. 357-367.
55. Faris, T.M., et al., *Developed simvastatin chitosan nanoparticles co-crosslinked with tripolyphosphate and chondroitin sulfate for ASGPR-mediated targeted HCC delivery with enhanced oral bioavailability.* Saudi Pharmaceutical Journal, 2020. **28**(12): p. 1851-1867.
56. Abdullah, T.A., N.J. Ibrahim, and M.H. Warsi, *Chondroitin sulfate-chitosan nanoparticles for ocular delivery of bromfenac sodium: Improved permeation, retention, and penetration.* International journal of pharmaceutical investigation, 2016. **6**(2): p. 96.
57. Nair, R.S., et al., *Matrix type transdermal patches of captopril: ex vivo permeation studies through excised rat skin.* Journal of Pharmacy Research, 2013. **6**(7): p. 774-779.
58. Agrawal, M.B. and M.M. Patel, *Optimization and in vivo evaluation of quetiapine-loaded transdermal drug delivery system for the treatment of schizophrenia.* Drug Development and Industrial Pharmacy, 2020. **46**(11): p. 1819-1831.
59. Verma, P. and S.S. Iyer, *Controlled Transdermal Delivery of Propranolol Using HPMC Matrices: Design and In-vitro and In-vivo Evaluation.* Journal of pharmacy and pharmacology, 2000. **52**(2): p. 151-156.
60. Malaiya, M.K., et al., *Controlled delivery of rivastigmine using transdermal patch for effective management of alzheimer's disease.* Journal of Drug Delivery Science and Technology, 2018. **45**: p. 408-414.
61. Chandak, A.R. and P.R.P. Verma, *Development and evaluation of HPMC based matrices for transdermal patches of tramadol.* Clinical Research and Regulatory Affairs, 2008. **25**(1): p. 13-30.
62. Singh, A. and A. Bali, *Formulation and characterization of transdermal patches for controlled delivery of duloxetine hydrochloride.* Journal of Analytical Science and Technology, 2016. **7**(1): p. 1-13.
63. Akhlaq, M., et al., *Formulation and evaluation of anti-rheumatic dexibuprofen transdermal patches: a quality-by-design approach.* Journal of drug targeting, 2016. **24**(7): p. 603-612.

64. Bernard, G., et al., *Physical characterization of the stratum corneum of an in vitro psoriatic skin model by ATR-FTIR and Raman spectroscopies.* Biochimica et Biophysica Acta (BBA)-General Subjects, 2007. **1770**(9): p. 1317-1323.
65. Binder, L., et al., *Penetration monitoring of drugs and additives by ATR-FTIR spectroscopy/tape stripping and confocal Raman spectroscopy–a comparative study.* European Journal of Pharmaceutics and Biopharmaceutics, 2018. **130**: p. 214-223.
66. Abdelwahed, W., et al., *Freeze-drying of nanoparticles: formulation, process and storage considerations.* Advanced drug delivery reviews, 2006. **58**(15): p. 1688-1713.
67. Zsikó, S., et al., *Methods to evaluate skin penetration in vitro.* Scientia Pharmaceutica, 2019. **87**(3): p. 19.
68. Babaei, S., et al., *Enhanced skin penetration of lidocaine through encapsulation into nanoethosomes and nanostructured lipid carriers: a comparative study.* Die Pharmazie-An International Journal of Pharmaceutical Sciences, 2016. **71**(5): p. 247-251.
69. Pena, A.-M., et al., *Imaging and quantifying drug delivery in skin–Part 2: Fluorescence andvibrational spectroscopic imaging methods.* Advanced drug delivery reviews, 2020. **153**: p. 147-168.
70. Makoni, P.A., K. Wa Kasongo, and R.B. Walker, *Short term stability testing of efavirenz-loaded solid lipid nanoparticle (SLN) and nanostructured lipid carrier (NLC) dispersions.* Pharmaceutics, 2019. **11**(8): p. 397.